Fig. 1. Effects of *in vivo* adaptive mutations on virus production in HuH-7 cells. One million cells were transfected with 10 μg *in vitro*-transcribed RNA of JFH-1/wt, JFH-1/S1, JFH-1/S2, and JFH-1/C. (A) HCV RNA and (B) core Ag levels in cell lysates and medium were measured at the indicated time points. Assays were performed in triplicate, and data are presented as the mean ± SD.

cation efficiency of these strains. However, the intracellular infectivity titers of JFH-1/C and JFH-1/S2 were 2.03 and 11.0 times higher than those of JFH-1/wt and JFH-1/S1, respectively ($P < 0.005$). Intracellular-specific infectivities (infectivity titer/HCV RNA copy number) of JFH-1/C and JFH-1/S2 showed more pronounced difference from those of JFH-1/wt and JFH-1/S1 (3.92 times and 12.9 times higher, respectively; $P < 0.005$). The infectious virus secretion rate (extracellular infectivity titer/intracellular infectivity titer) was not significantly different between JFH-1/wt and variant strains. These data indicate that mutations identified in chimpanzees at the later time point of infection led to reduced viral replication and increased assembly of infectious virus particles without any effect on viral release in cell culture.

Subgenomic Replicon Assay. To further confirm the replication efficiencies of strains observed in chimpanzees, we generated subgenomic replicons of JFH-1/wt, JFH-1/S1, JFH-1/S2, and JFH-1/C carrying the firefly luciferase reporter gene (SGR-JFH-1/Luc/wt, SGR-JFH-1/Luc/S1, SGR-JFH-1/Luc/S2, and SGR-JFH-1/Luc/C). *In vitro*-transcribed RNAs of these constructs were transfected into HuH-7 cells, and luciferase activity was measured to assess their replication capacity. The luciferase activities of SGR-JFH-1/Luc/C and SGR-JFH-1/Luc/S2 replicons were 7.30 and 7.33 times lower than those of SGR-JFH-1/Luc/wt and SGR-JFH-1/Luc/S1, respectively, at day 1 ($P < 0.00005$), suggesting attenuated replication capacities of variant replicons isolated from each animal at later time points of infection (Supporting Fig. 1A). The luciferase activity 4 hours after transfection was comparable, indicating similar levels of transfection efficiency (data not shown). Based on these data, we found that the mutations that emerged in nonstructural (NS)3-NS5B of JFH-1/S2 and JFH-1/C reduced the replication efficiency in cell culture.

Genomic Regions Responsible for Lower Replication and Higher Assembly of JFH-1/S2. To further clarify the genomic region responsible for lower replication efficiency and higher assembly rate of JFH-1/S2, we generated the chimeric constructs JFH-1/S2-wt and JFH-1/wt-S2 as described in the Supporting Materials and Methods. *In vitro*-transcribed RNAs of JFH-1/wt, JFH-1/S2, JFH-1/S2-wt, and JFH-1/wt-S2 were introduced into HuH-7 cells by electroporation and intracellular and extracellular HCV RNA and core Ag were measured. At day 5 posttransfection, all constructs displayed comparable intracellular HCV RNA levels (Fig. 2). However, extracellular HCV RNA levels of JFH-1/S2 and JFH-1/S2-wt were significantly

line that lacks the surface expression of CD81, one of the cellular receptors for HCV entry. Three days after transfection with full-genome RNA of JFH-1/wt, JFH-1/S1, JFH-1/S2, and JFH-1/C, HCV RNA levels and infectivity titer were measured, and the specific infectivity was calculated (Table 1). Intracellular HCV RNA levels of JFH-1/C and JFH-1/S2 were lower than those of JFH-1/wt and S1, suggesting lower repli-

Table 1. Infectious Virus Production and Release of JFH-1/wt and Variants in Huh7-25 Cells

| Strain | Intracellular | | | Extracellular | Secretion Ratio (Extracellular/Intracellular) |
	HCV RNA (copies/μg RNA)	Infectivity Titer (ffu/well)	Specific Infectivity (ffu/copies)	Infectivity Titer (ffu/well)	
JFH-1/wt	$7.75 \times 10^8 \pm 1.04 \times 10^8$	$4.21 \times 10^2 \pm 4.32 \times 10^1$	$2.09 \times 10^{-7} \pm 7.06 \times 10^{-8}$	$1.94 \times 10^3 \pm 3.76 \times 10^1$	4.6 ± 1.3
JFH-1/S1	$7.04 \times 10^8 \pm 8.49 \times 10^7$	$4.72 \times 10^2 \pm 5.63 \times 10^1$	$2.91 \times 10^{-7} \pm 6.00 \times 10^{-8}$	$3.02 \times 10^3 \pm 2.77 \times 10^2$	5.4 ± 2.0
JFH-1/S2	$4.16 \times 10^{8**} \pm 7.47 \times 10^6$	$5.19 \times 10^{3**} \pm 8.24 \times 10^1$	$3.76 \times 10^{-6**} \pm 7.01 \times 10^{-7}$	$3.23 \times 10^{4**} \pm 3.52 \times 10^3$	6.2 ± 3.0
JFH-1/C	$3.15 \times 10^{8*} \pm 5.02 \times 10^7$	$8.59 \times 10^{2*} \pm 4.81 \times 10^1$	$8.19 \times 10^{-7*} \pm 5.68 \times 10^{-8}$	$3.68 \times 10^3 \pm 3.02 \times 10^3$	4.3 ± 1.4
JFH-1/S2-wt	$7.07 \times 10^8 \pm 8.43 \times 10^7$	$4.40 \times 10^{3*} \pm 9.5 \times 10^1$	$2.73 \times 10^{-6*} \pm 2.35 \times 10^{-7}$	$3.0 \times 10^{4*} \pm 1.1 \times 10^3$	6.7 ± 0.7
JFH-1/wt-S2	$4.21 \times 10^{8*} \pm 1.97 \times 10^7$	$2.7 \times 10^2 \pm 2.9 \times 10^1$	$2.02 \times 10^{-7} \pm 4.0 \times 10^{-8}$	$1.7 \times 10^3 \pm 1.3 \times 10^2$	4.5 ± 0.4

Abbreviation: ffu, focus-forming units.
*$P < 0.005$ versus JFH-1/wt.
**$P < 0.005$ versus JFH-1/S1.

higher ($P < 0.0005$) than that of JFH-1/wt. On the other hand, extracellular RNA level of JFH-1/wt-S2 chimeric construct was lower than that of JFH-1/S2 and JFH-1/S2-wt and similar to that of JFH-1/wt. Likewise, extracellular core Ag levels of JFH-1/S2 and JFH-1/S2-wt were also significantly higher than that of JFH-1/wt. Intracellular HCV core Ag levels of JFH-1/S2 and JFH-1/wt-S2 on day 1 posttransfection were 240.9 ± 58.2 and 134.3 ± 17.1 fmol/mg protein, respectively, and were significantly lower ($P < 0.005$) than that of JFH-1/wt (526.1 ± 58.2 fmol/mg protein), whereas intracellular HCV core Ag level of JFH-1/S2-wt was comparable to that of JFH-1/wt. Transfection efficiency of these strains, indicated by intracellular HCV core Ag levels at 4 hours posttransfection, was almost identical (data not shown).

To further elucidate, we transfected Huh7-25 cells with *in vitro*–transcribed RNA of JFH-1/wt, JFH-1/S2, JFH-1/S2-wt, and JFH-1/wt-S2 and measured HCV RNA, core Ag, and infectivity titer in the cells and culture medium. Intracellular HCV RNA levels of JFH-1/S2 and JFH-1/wt-S2 were similar and lower than those of JFH-1/wt and JFH-1/S2-wt, suggesting mutations in NS3-NS5B were responsible for lower replication efficiency of JFH-1/S2 (Table 1). Intracellular infectivity titer of JFH-1/S2 and JFH-1/S2-wt was 12.3 and 10.4 times higher, respectively, than that of JFH-1/wt ($P < 0.005$) on day 3 posttransfection. The intracellular specific infectivities of JFH-1/S2 and JFH-1/S2-wt were significantly higher than that of JFH-1/wt (18 times and 13.1 times higher, respectively; $P < 0.005$). On the other hand, intracellular specific infectivity of JFH-1/wt-S2 was comparable to that of JFH-1/wt. The infectious virus secretion rate was not significantly different among all the constructs (Table 1). These data indicate that mutations emerged in the core-NS2 region of JFH-1/S2 are responsible

for the enhanced assembly of infectious virus particles compared with JFH-1/wt.

Mapping Study for JFH-1/S2 Strain. Because our experiments with JFH-1/S2 subgenomic replicon and JFH-1/wt-S2 chimeric construct showed that mutations emerged in the NS3-NS5B region are responsible for reduced replication efficiency of JFH-1/S2, we performed mapping studies by generating various JFH-1 subgenomic replicons, each containing the mutations observed in individual nonstructural protein. Although mutations in NS4B and NS5A were associated with attenuated replication capacity of JFH-1, the most significant decrease in replication was observed with NS5B mutations (Supporting Fig. 1B).

For detailed analysis of mutations responsible for higher assembly, *in vitro*–transcribed RNAs of JFH-1/wt, JFH-1/S2, JFH-1/S2-wt, JFH-1/N397S, JFH-1/L752V, JFH-1/S2-NS2 (containing mutations G838R, A878V, and V881A), JFH-1/G838R, and JFH-1/A878V were transfected into Huh7-25 cells, and intracellular-specific infectivities were compared (Supporting Table 2). As reported previously, JFH1/G838R showed higher intracellular specific infectivity than that of JFH-1/wt, but could not reach the level of JFH-1/S2 or JFH-1/S2-wt. Among the mutants, intracellular specific infectivities of JFH1/L752V, JFH1/NS2, and JFH1/G838R were 4.02, 5.42, and 3.07 times higher than that of JFH-1/wt, but those of JFH1/N397S and JFH1/A878V were similar to that of JFH-1/wt. Thus, the combination of mutations in P7 and NS2 was found to contribute to the higher assembly of the JFH-1/S2 strain.

Human Hepatocyte–Transplanted Mouse Assay. To assess the *in vivo* infectivity of these strains, we inoculated culture medium containing 10^7 copies (HCV RNA titer measured by RTD-PCR) of JFH-1/wt, JFH-1/S1, JFH-1/S2, and C viruses into human
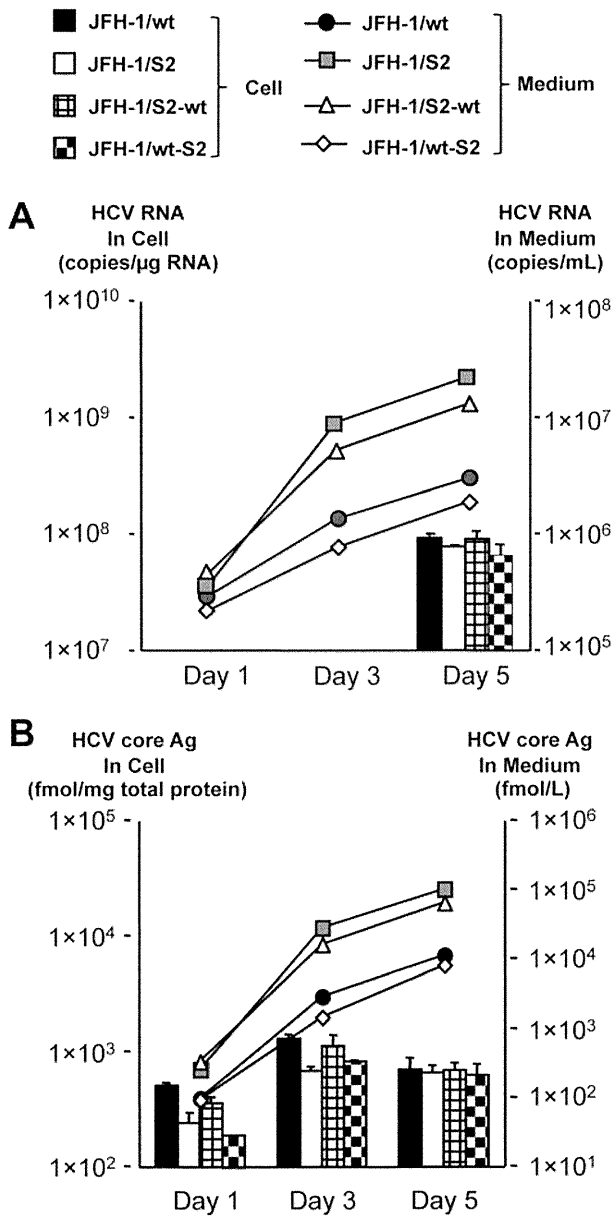
Cell
- ■ JFH-1/wt
- □ JFH-1/S2
- ⊞ JFH-1/S2-wt
- ▨ JFH-1/wt-S2

Medium
- —●— JFH-1/wt
- —■— JFH-1/S2
- —△— JFH-1/S2-wt
- —◇— JFH-1/wt-S2

A

HCV RNA
In Cell
(copies/µg RNA)

HCV RNA
In Medium
(copies/mL)

Day 1   Day 3   Day 5

B

HCV core Ag
In Cell
(fmol/mg total protein)

HCV core Ag
In Medium
(fmol/L)

Day 1   Day 3   Day 5

Fig. 2. Virus production of JFH-1/S2 chimeric constructs in HuH-7 cells. One million cells were transfected with 10 µg in vitro–transcribed RNA of JFH-1/wt, JFH-1/S2, JFH-1/S2-wt, and JFH-1/wt-S2. (A) HCV RNA and (B) core Ag levels in cell lysates and medium were measured at the indicated time points. Assays were performed in triplicate, and data are presented as the mean ± SD.

infected HCV RNA titer among these inoculated mice. Sequence analyses of the complete open reading frames revealed that infecting JFH-1/wt virus and variant strains had no nonsynonymous mutations at the time of development of infection. From these data, we concluded that not only JFH-1/wt virus but also JFH-1/S1, JFH-1/S2, and JFH-1/C viruses were able to establish productive infection in human hepatocyte-transplanted mice.

Apoptosis Induction Assay. To investigate the survival strategy against the host defense system, we examined the susceptibility of JFH-1/wt and variant strains to TNF-α–mediated apoptosis induction. After transfection with in vitro–transcribed RNA of JFH-1/wt, JFH-1/S1, JFH-1/S2, and JFH-1/C, Huh-7.5.1 cells were exposed to TNF-α plus actinomycin D. Without exposure, apoptosis was observed in a limited number of HCV-positive cells (Supporting Fig. 2A). Forty-eight hours later, cells were harvested, fixed, and
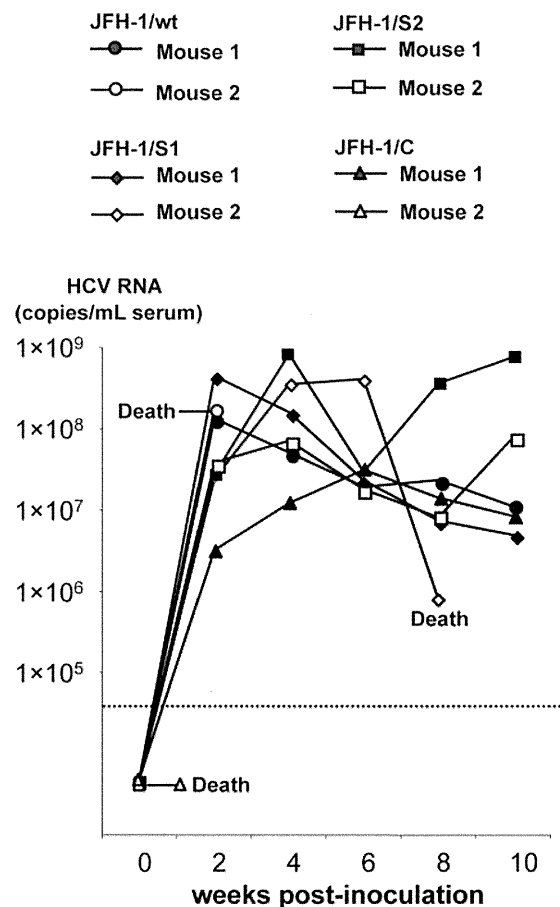
JFH-1/wt
- —●— Mouse 1
- —○— Mouse 2

JFH-1/S2
- —■— Mouse 1
- —□— Mouse 2

JFH-1/S1
- —◆— Mouse 1
- —◇— Mouse 2

JFH-1/C
- —▲— Mouse 1
- —△— Mouse 2

HCV RNA
(copies/mL serum)

Death

Death

Death

weeks post-inoculation

Fig. 3. In vivo infection study of JFH-1/wt and its variants in human hepatocyte-transplanted mice. Cell culture medium containing 1 × 10^{7} HCV RNA copies of JFH-1/wt, JFH-1/S1, JFH-1/S2, and JFH-1/C were inoculated into human hepatocyte–transplanted mice, and HCV RNA levels in mice serum were monitored.

hepatocyte-transplanted mice. Two mice were used for each virus. Two weeks after intravascular inoculation, all mice but one became HCV RNA–positive (Fig. 3). Two mice died 3 weeks after inoculation; one was inoculated with JFH-1/wt and had developed infection, and the other was inoculated with JFH-1/C and died without developing infection. HCV RNA levels in infected mice fluctuated, ranging from 10^6 to 10^9 copies/mL. We could not observe much difference of

subjected to terminal deoxynucleotidyl transferase–mediated deoxyuridine triphosphate nick-end labeling (TUNEL) assay and anti-HCV NS5A staining. The effects of JFH-1/wt, JFH-1/S1, JFH-1/S2, and JFH-1/C transfection on apoptosis induction were determined by calculating the ratio of apoptosis between HCV-positive and HCV-negative populations and expressed as an apoptosis induction index. After treatment of JFH-1/wt–transfected cells with TNF-α, apoptosis was observed in 36.8% of the HCV-positive population and in 19.3% of the HCV-negative population, and the apoptosis induction index was 1.85 ± 0.06 (Fig. 4). The apoptosis induction indexes of JFH-1/S1–transfected and JFH-1/C– transfected cells were 1.23 ± 0.06 and 1.16 ± 0.10, respectively, suggesting lower susceptibility to apoptosis induction compared with JFH-1/wt. On the other hand, the apoptosis induction index of JFH-1/S2 was 0.74 ± 0.17, which was substantially lower than that of JFH-1/wt, demonstrating the more reduced apoptosis in the cells harboring this strain. Similar results were obtained by treatment with FasL plus actinomycin D (Supporting Fig. 2B). To confirm the lower susceptibility of JFH-1/S2–transfected cells, apoptosis was also detected by staining with anticleaved poly(adenosine diphosphate ribose) polymerase (PARP) antibody. The apoptosis induction indexes of JFH-1/wt and JFH-1/S2–transfected cells were 2.28 ± 0.24 and 1.15 ± 0.14, respectively, and were consistent with TUNEL assay (Fig. 5). Although the HCV NS5A-positive rate in JFH-1/S2–transfected cells was higher than that in JFH-1/wt, the mean fluorescence intensity of the NS5A-positive population in JFH-1/S2–transfected cells was significantly lower (185.0 ± 8.7) than that in JFH-1/wt–transfected cells (395.0 ± 98.0), corresponding to the observed phenotype of the JFH-1/S2 strain in the single cycle virus production assay (i.e., lower replication efficiency and rapid spread to surrounding cells).

To clarify the genomic region responsible for lower susceptibility of JFH-1/S2 to cytokine-induced apoptosis, we examined the effect of TNF-α on the cells carrying subgenomic reporter replicons. The apoptosis induction index of SGR-JFH1/Luc/S2–transfected cells was lower than that of SGR-JFH1/Luc/wt–transfected cells (Supporting Fig. 2C); however, the difference was not as pronounced as with full-genome constructs, indicating that mutations in the NS3-NS5B region contribute to lower susceptibility of JFH-1/S2 to cytokine-induced apoptosis, but they are not sufficient to explain the difference between JFH-1/wt and JFH-1/S2. We confirmed these results by use of the chimeric
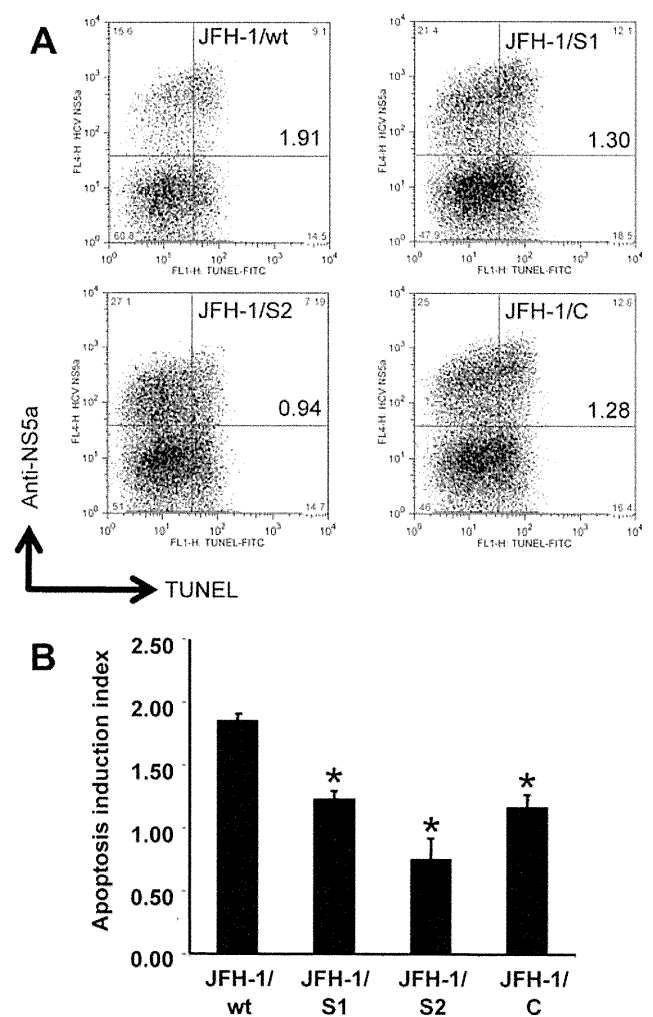

Fig. 4. Apoptosis induction in Huh-7.5.1 cells transfected with JFH-1/wt and its variants. (A) Three million cells were transfected with 3 μg in vitro-transcribed full-genome RNA of JFH-1/wt, JFH-1/S1, JFH-1/S2, and JFH-1/C. Forty-eight hours later, apoptosis was induced by exposing cells to 20 ng/mL TNF-α plus 50 ng/mL actinomycin D. Cells were harvested after 48 hours of treatment and subjected to TUNEL and anti-HCV NS5A staining. Dot plots show HCV replication and apoptosis at the single cell level. Quadrant gates were determined using unstained and a terminal deoxynucleotidyltrasferase-untreated control in each culture condition. The clone names and apoptosis induction indexes are indicated in the upper right box. (B) Apoptosis induction indexes of JFH-1/wt-, JFH-1/S1-, JFH-1/S2-, and JFH-1/C- transfected cells. The mean ± SD of three independent experiments is shown. *P < 0.005 versus JFH-1/wt.

constructs JFH-1/S2-wt and JFH-1/wt-S2. The apoptosis induction indexes of JFH-1/S2-wt–transfected and JFH-1/wt-S2–transfected cells were 1.42 ± 0.13 and 1.71 ± 0.08, respectively (Fig. 5). These data indicate that both structural and nonstructural regions of JFH-1/S2 were associated with lower susceptibility to cytokine-induced apoptosis, although mutations in core-NS2 seemed to have higher contribution toward this phenotype. Together, these results indicate that the JFH-1/S2 strain, which was selected after passage in
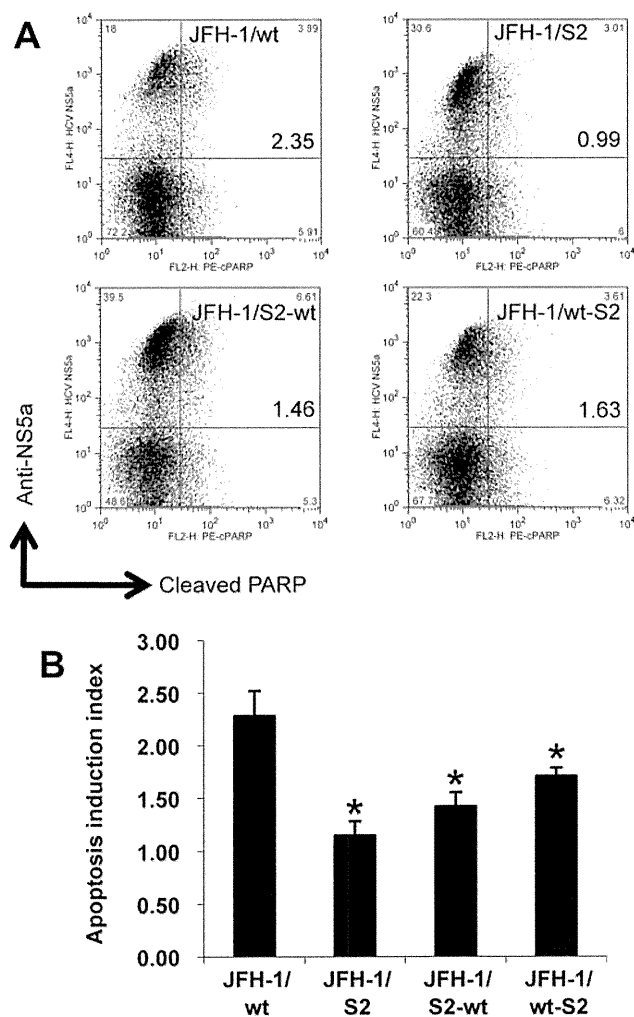
A

Cleaved PARP

B

Fig. 5. Apoptosis induction in Huh-7.5.1 cells transfected with JFH-1/wt, JFH-1/S2, and their chimeric constructs. (A) Three million cells were transfected with 3 μg in vitro-transcribed full-genome RNA of JFH-1/wt, JFH-1/S2, JFH-1/S2-wt, and JFH-1/wt-S2. Apoptosis was induced by exposing cells to 20 ng/mL TNF-α plus 50 ng/mL actinomycin D and detected by anticleaved PARP staining. The clone names and apoptosis induction indexes are indicated in the upper right box. (B) Apoptosis induction indexes of JFH-1/wt-, JFH-1/S2-, JFH-1/S2-wt-, and JFH-1/wt-S2-transfected cells. The mean ± SD of three independent experiments is shown. *P < 0.05 versus JFH-1/wt.

the patient serum–infected chimpanzee, acquired less susceptibility to the cytokine-induced apoptosis.

Discussion

HCV develops chronic infection in the vast majority of infected patients[1]; however, the mechanisms of its persistence are still under investigation. Many viruses have evolved different strategies to cope with host immune systems, thus causing the development of persistent infection. For example, some viruses interfere with the major histocompatibility complex class I presentation of viral antigens, whereas others modulate

lymphocyte and macrophage functions, including cytokine production.[12-16] In our previous study, we detected an increasing number of mutations in the HCV genome isolated from JFH-1 patient serum–infected chimpanzees. Thus, we reasoned that these detected mutations might have imparted some advantage to this virus for long-time survival. To examine this hypothesis, we compared the phenotypes of JFH-1 variant strains emerged at early and late stages of infection in JFH-1 patient serum–infected and JFH-1cc–infected chimpanzees and found that the JFH-1/S2 strain isolated from the patient serum–infected chimpanzee at a later time point of infection replicated slowly, produced more infectious viruses, and displayed reduced susceptibility to cytokine-induced apoptosis.

The JFH-1 variant strain JFH-1/C, which contains seven nonsynonymous mutations identified in the JFH-1cc–infected chimpanzee at week 7, showed comparatively slower replication kinetics and slightly enhanced infectious virus production in cell culture. The intracellular specific infectivity of this strain in Huh7-25 cells was 3.9 times higher than that of JFH-1/wt (Table 1). These characteristics might have imparted some advantage to this strain for establishing productive infection in the chimpanzee. The other JFH-1 variant strains, JFH-1/S1 and JFH-1/S2, contain 6 and 17 nonsynonymous mutations identified in the JFH-1 patient serum–infected chimpanzee at weeks 2 and 23 postinfection, respectively. Replication kinetics and infectious virus production of the JFH-1/S1 strain were comparable to that of JFH-1/wt in cultured cells (Fig. 1, Table 1). In contrast, the JFH-1/S2 strain showed lower replication efficiency. Although the intracellular HCV RNA level of this strain in Huh7-25 cells was lower than that of JFH-1/wt and JFH-1/S1, and almost the same as that of JFH-1/C (Table 1), intracellular specific infectivity was 18.0 and 12.9 times higher than that of JFH-1/wt and JFH-1/S1, respectively, suggesting a significant increase in the assembly of infectious virus particles (P < 0.005, Table 1). The enhanced capacity of this strain to assemble infectious virus particles resulted in a higher extracellular infectivity titer that contributed to the rapid spread of virus to surrounding cells. Flow cytometry analyses of cells transfected with JFH-1/wt and variant strains revealed that the percentage of the HCV NS5A-positive population in JFH-1/S2–transfected cells was higher, but the mean fluorescence intensity of the anti-NS5A signal was lower than that in JFH-1/wt–transfected cells, thus confirming higher spread and lower replication of this strain. Taken together, both JFH-1/C and JFH-1/S2 exhibited a tendency toward

decreased replication and increased infectious virus production. However, the extent of enhanced virus production was substantially lower in JFH-1/C than in JFH-1/S2, which might have led to the earlier elimination of infection in the JFH-1cc–infected chimpanzee. In other words, the potency of infectious virus production and spread seems to correspond to the duration of infection in infected animals.

The association between a lower replication efficiency and persistent infection is still unclear. It has been reported that an escape mutant with an amino acid substitution at the cytotoxic T lymphocyte (CTL) epitope in the NS3 region exhibits lower NS3/4 protease activity and replication capacity *in vitro*.[17,18] The JFH-1/S2 strain contains the T1077A mutation in the NS3 region (Supporting Table 1), and this mutation is located close to mutations reported to be associated with immune evasion and lower replication.[17] Thus, the lower replication efficiency of the JFH-1/S2 strain may be a result of an immune escape mutation at the expense of viral fitness. Meanwhile, we cannot deny the advantage of lower replication in establishing persistent infection. Lower replication may contribute to the avoidance of major histocompatibility class I–mediated antigen presentation and to escape from the host immune system. Either way, by acquiring the ability to produce more viral particles, the JFH-1/S2 strain could rapidly spread to surrounding cells, irrespective of its lower replication efficiency. Importantly, these emerged mutations did not attenuate *in vivo* infectivity, unlike cell culture adaptive mutations reported to cause attenuated infection *in vivo*.[19] Upon inoculation into human hepatocyte–transplanted mice, JFH-1/S1, JFH-1/S2, and JFH-1/C strains could establish infection without any mutations, produced levels of viremia similar to JFH-1/wt, and persisted for a similar observed period of infection (Fig. 2). This observation is different from that in chimpanzees, where JFH-1/wt and JFH-1/C strains were eliminated earlier than JFH-1/S2. In contrast to chimpanzees, human hepatocyte–transplanted mice lack a CTL and natural killer (NK) cell–mediated immune system, which could be responsible for this difference.[6] Taken together, our results suggest that along with efficient infectious virus production, the JFH-1/S2 strain might have acquired an advantage that helps it evade the CTL and NK cell–mediated immune system.

Apoptosis of virus-infected cells by the immune system is crucial as a general mechanism of clearing infections.[20,21] The J6/JFH-1 chimeric virus has been reported to exhibit proapoptotic characteristics in cell culture.[22] However, because HCV needs to escape the host immune system in order to establish chronic infection, immune cell–mediated apoptosis may be inhibited in infected hepatocytes. In the liver, HCV-infected hepatocytes are eliminated by targeted apoptosis induced by NK cells, macrophages, and CTLs with ligand-mediated and receptor-mediated signals such as TNF-α, FasL, and TNF-related apoptosis–inducing ligand.[23-26] Thus, we used TNF-α to mimic natural immunomediated apoptosis and found that the JFH-1/S2–replicating cells have lower susceptibility to the apoptosis induced by these cytokines. In JFH-1/S2–transfected cells, TNF-α–induced apoptosis detected by TUNEL assay was substantially lower than that of JFH-1/wt–transfected cells (Fig. 4). We confirmed it by staining with anticleaved PARP. In complete agreement with the results produced by way of TUNEL assay, the number of anticleaved PARP stained cells among JFH-1/S2–infected cells was significantly lower than that among JFH-1/wt–infected cells (Fig. 5). In our previous study, we reported that HCV-specific immune responses with T cell proliferation and interferon-γ production were maintained until the disappearance of viremia in the patient serum–infected chimpanzee.[11] This finding indicates that continuous selection pressure in the infected chimpanzee might have contributed to the emergence of a clone with an ability to escape the cytokine-induced apoptosis. We are not sure whether this phenotype of JFH-1/S2 is due to its lower replication efficiency and thus lower production of HCV proteins. The accumulation of viral proteins might predispose cells to the apoptosis induced by TNF-α. To answer this question, it will be necessary to investigate the genomic regions of JFH-1/S2 and cellular host factors responsible for the ability of this strain to escape the apoptosis.

By way of mapping analysis for JFH-1/S2, we could determine responsible regions; NS5B was for lower replication efficiency (Supporting Fig. 1B), and P7 and NS2 were for enhanced viral particle assembly (Supporting Table 2). For the evasion of apoptosis, we could not specify the responsible region, because both chimeric constructs, JFH-1/S2-wt and JFH-1/wt-S2, showed less susceptibility to cytokine-induced apoptosis to a certain extent. These data indicate that both structural and nonstructural regions might have contributed to the acquisition of this phenotype. Previously, a potent antiapoptotic effect of the HCV NS5A protein was described.[27] NS5A interacts with Bin1, which is a nucleocytoplasmic c-Myc–interacting protein with tumor suppressor and apoptotic properties, thus inhibiting Bin1-

associated apoptosis. Because JFH-1/S2 contains several mutations in the NS5A region (Supporting Table 1), one or more mutations in this protein may be associated with antiapoptotic effects.

In conclusion, we demonstrated that the JHF-1/S2 strain acquired phenotypes of lower replication, higher virus production, and less susceptibility to cytokine-induced apoptosis. These phenotypes were associated with mutations that emerged 23 weeks after infection in a chimpanzee, and might have contributed to long-term infection *in vivo*. Such control of viral functions by specific mutations may be a key viral strategy to establish persistent infection.

References

1. Liang TJ, Rehermann B, Seeff LB, Hoofnagle JH. Pathogenesis, natural history, treatment, and prevention of hepatitis C. Ann Intern Med 2000;132:296-305.
2. Feld JJ, Liang TJ. Hepatitis C—identifying patients with progressive liver injury. HEPATOLOGY 2006;43:S194-S206.
3. Thimme R, Oldach D, Chang KM, Steiger C, Ray SC, Chisari FV. Determinants of viral clearance and persistence during acute hepatitis C virus infection. J Exp Med 2001;194:1395-1406.
4. Thimme R, Bukh J, Spangenberg HC, Wieland S, Pemberton J, Steiger C, et al. Viral and immunological determinants of hepatitis C virus clearance, persistence, and disease. Proc Natl Acad Sci U S A 2002;99: 15661-15668.
5. Mercer DF, Schiller DE, Elliott JF, Douglas DN, Hao C, Rinfret A, et al. Hepatitis C virus replication in mice with chimeric human livers. Nat Med 2001;7:927-933.
6. Tateno C, Yoshizane Y, Saito N, Kataoka M, Utoh R, Yamasaki C, et al. Near completely humanized liver in mice shows human-type metabolic responses to drugs. Am J Pathol 2004;165:901-912.
7. Kato T, Furusaka A, Miyamoto M, Date T, Yasui K, Hiramoto J, et al. Sequence analysis of hepatitis C virus isolated from a fulminant hepatitis patient. J Med Virol 2001;64:334-339.
8. Wakita T, Pietschmann T, Kato T, Date T, Miyamoto M, Zhao Z, et al. Production of infectious hepatitis C virus in tissue culture from a cloned viral genome. Nat Med 2005;11:791-796.
9. Zhong J, Gastaminza P, Cheng G, Kapadia S, Kato T, Burton DR, et al. Robust hepatitis C virus infection in vitro. Proc Natl Acad Sci U S A 2005;102:9294-9299.
10. Lindenbach BD, Evans MJ, Syder AJ, Wolk B, Tellinghuisen TL, Liu CC, et al. Complete replication of hepatitis C virus in cell culture. Science 2005;309:623-626.
11. Kato T, Choi Y, Elmowalid G, Sapp RK, Barth H, Furusaka A, et al. Hepatitis C virus JFH-1 strain infection in chimpanzees is associated with low pathogenicity and emergence of an adaptive mutation. HEPATOLOGY 2008;48:732-740.
12. Johannessen I, Crawford DH. In vivo models for Epstein-Barr virus (EBV)-associated B cell lymphoproliferative disease (BLPD). Rev Med Virol 1999;9:263-277.
13. Oglesbee MJ, Pratt M, Carsillo T. Role for heat shock proteins in the immune response to measles virus infection. Viral Immunol 2002;15: 399-416.
14. Stevenson PG, Boname JM, de Lima B, Efstathiou S. A battle for survival: immune control and immune evasion in murine gamma-herpesvirus-68 infection. Microbes Infect 2002;4:1177-1182.
15. Alcami A. Viral mimicry of cytokines, chemokines and their receptors. Nat Rev Immunol 2003;3:36-50.
16. Wilkinson GW, Tomasec P, Stanton RJ, Armstrong M, Prod'homme V, Aicheler R, et al. Modulation of natural killer cells by human cytomegalovirus. J Clin Virol 2008;41:206-212.
17. Soderholm J, Ahlen G, Kaul A, Frelin L, Alheim M, Barnfield C, et al. Relation between viral fitness and immune escape within the hepatitis C virus protease. Gut 2006;55:266-274.
18. Uebelhoer L, Han JH, Callendret B, Mateu G, Shoukry NH, Hanson HL, et al. Stable cytotoxic T cell escape mutation in hepatitis C virus is linked to maintenance of viral fitness. PLoS Pathog 2008;4: e1000143.
19. Bukh J, Pietschmann T, Lohmann V, Krieger N, Faulk K, Engle RE, et al. Mutations that permit efficient replication of hepatitis C virus RNA in Huh-7 cells prevent productive replication in chimpanzees. Proc Natl Acad Sci U S A 2002;99:14416-14421.
20. Kagi D, Seiler P, Pavlovic J, Ledermann B, Burki K, Zinkernagel RM, et al. The roles of perforin- and Fas-dependent cytotoxicity in protection against cytopathic and noncytopathic viruses. Eur J Immunol 1995;25:3256-3262.
21. Kagi D, Vignaux F, Ledermann B, Burki K, Depraetere V, Nagata S, et al. Fas and perforin pathways as major mechanisms of T cell-mediated cytotoxicity. Science 1994;265:528-530.
22. Deng L, Adachi T, Kitayama K, Bungyoku Y, Kitazawa S, Ishido S, et al. Hepatitis C virus infection induces apoptosis through a Bax-triggered, mitochondrion-mediated, caspase 3-dependent pathway. J Virol 2008;82:10375-10385.
23. Kafrouni MI, Brown GR, Thiele DL. Virally infected hepatocytes are resistant to perforin-dependent CTL effector mechanisms. J Immunol 2001;167:1566-1574.
24. Guicciardi ME, Gores GJ. Apoptosis: a mechanism of acute and chronic liver injury. Gut 2005;54:1024-1033.
25. Fischer R, Baumert T, Blum HE. Hepatitis C virus infection and apoptosis. World J Gastroenterol 2007;13:4865-4872.
26. Stegmann KA, Bjorkstrom NK, Veber H, Ciesek S, Riese P, Wiegand J, et al. Interferon-alpha-induced TRAIL on natural killer cells is associated with control of hepatitis C virus infection. Gastroenterology 2010; 138:1885-1897.
27. Nanda SK, Herion D, Liang TJ. The SH3 binding motif of HCV NS5A protein interacts with Bin1 and is important for apoptosis and infectivity. Gastroenterology 2006;130:794-809.

Malnutrition Impairs Interferon Signaling Through mTOR and FoxO Pathways in Patients With Chronic Hepatitis C

MASAO HONDA,*,‡ KENJI TAKEHANA,§ AKITO SAKAI,* YUSUKE TAGATA,§ TAKAYOSHI SHIRASAKI,‡
SHINOBU NISHITANI,§ TAKAHIKO MURAMATSU,∥ TATSUYA YAMASHITA,* YASUNARI NAKAMOTO,*
EISHIRO MIZUKOSHI,* YOSHIO SAKAI,* TARO YAMASHITA,* MIKIKO NAKAMURA,* TETSURO SHIMAKAMI,¶
MINKYUNG YI,# STANLEY M. LEMON,¶ TETSUO SUZUKI,** TAKAJI WAKITA,** SHUICHI KANEKO,* and the Hokuriku Liver
Study Group

*Department of Gastroenterology, ‡Department of Advanced Medical Technology, Kanazawa University Graduate School of Medicine, Kanazawa, Japan; §Exploratory
Research Laboratories, Research Center, Ajinomoto Pharmaceuticals, Co, Ltd, Kanagawa, Japan; ∥Frontier Research Labs, Institute for Innovation, Ajinomoto, Co,
Inc, Kanagawa, Japan; ¶Division of Infectious Diseases, School of Medicine, The University of North Carolina at Chapel Hill, Chapel Hill, North Carolina; #Center for
Hepatitis Research, Institute for Human Infections and Immunity, and Department of Microbiology and Immunology, University of Texas Medical Branch, Galveston,
Texas; and **Department of Virology II, National Institute of Infectious Diseases, Tokyo, Japan

BACKGROUND & AIMS: Patients with advanced chronic hepatitis C (CH-C) often are malnourished, but the effects of malnutrition on interferon (IFN) signaling and response to treatment have not been determined. We assessed the importance of the nutritional state of the liver on IFN signaling and treatment response. **METHODS:** We studied data from 168 patients with CH-C who were treated with the combination of pegylated-IFN and ribavirin. Plasma concentrations of amino acids were measured by mass spectrometry. Liver gene expression profiles were obtained from 91 patients. Huh-7 cells were used to evaluate the IFN signaling pathway, mammalian target of rapamycin complex 1 (mTORC1), and forkhead box O (FoxO). Antiviral signaling induced by branched-chain amino acids (BCAAs) was determined using the in vitro hepatitis C virus replication system. **RESULTS:** Multivariate logistic regression analysis showed that Fischer's ratio was associated significantly with nonresponders, independent of interleukin-28B polymorphisms or the histologic stage of the liver. Fischer's ratio was correlated inversely with the expression of BCAA transaminase 1, and was affected by hepatic mTORC1 signaling. IFN stimulation was impaired substantially in Huh-7 cells grown in medium that was low in amino acid concentration, through repressed mTORC1 signaling, and increased Socs3 expression, which was regulated by Foxo3a. BCAA could restore impaired IFN signaling and inhibit hepatitis C virus replication under conditions of malnutrition. **CONCLUSIONS:** Malnutrition impaired IFN signaling by inhibiting mTORC1 and activating Socs3 signaling through Foxo3a. Increasing BCAAs to up-regulate IFN signaling might be used as a new therapeutic approach for patients with advanced CH-C.

Keywords: HCV; Liver Disease; Therapy; Diet.

Interferon (IFN) and ribavirin (RBV) combination therapy is a popular modality for treating patients with chronic hepatitis C (CH-C), but approximately 50% of patients usually relapse, particularly those with hepatitis C virus (HCV) genotype 1b and a high viral load.[1]

Recent landmark studies of genome-wide associations identified genomic loci associated with treatment responses to pegylated (Peg)-IFN and RBV combination therapy,[2,3] and a polymorphism in the interleukin (IL)-28B gene was found to predict hepatitis C treatment-induced viral clearance. Moreover, we previously showed that expression of hepatic IFN-stimulated genes (ISGs) was associated with the IL-28B polymorphism and might contribute to the treatment response.[4] In addition to the IL-28B polymorphism, host factors such as fibrosis stage and metabolic status of the liver might be associated with the treatment outcome[4,5]; however, the significance of these factors in conjunction with the IL-28B polymorphism has not been evaluated fully.

In CH-C livers, prolonged liver cell damage, fibrosis development, and microcirculation failure can lead to a state of malnutrition in hepatocytes, resulting in the impairment of multiple metabolic pathways. In patients with advanced stage CH-C, hypoalbuminemia and decreased plasma values for the Fischer's ratio of branched-amino acids (BCAA; leucine, isoleucine, and valine) to aromatic amino acids (tyrosine and phenylalanine) commonly are observed. BCAA are the essential amino acids necessary for ammonium metabolism in muscle when the liver is unable to perform this function. Recent reports have shown that BCAA activates albumin synthesis in rat

primary hepatocytes[6] and cirrhotic rat liver[7] through mammalian target of rapamycin (mTOR) signaling, a central regulator of protein synthesis, by sensing nutrient conditions.[8] Thus, peripheral amino acid composition is closely related to signaling pathways in the liver.

In addition to metabolic aspects, recent reports have elucidated new functional roles for mTOR in the IFN signaling pathway. Targeted disruptions of tuberous sclerosis 2 and eukaryotic translation initiation factor 4E binding protein 1, which both inhibit mTOR complex 1 (mTORC1) signaling, substantially enhanced IFN-alfa–dependent antiviral responses.[9,10] Therefore, mTORC1 signaling might be involved in the antiviral response as well as in metabolic processes. However, these issues have not yet been addressed in terms of IFN treatment for CH-C. In the present study, therefore, we evaluated the clinical relevance of the nutritional state of the liver, as estimated by the plasma Fischer's ratio, on Peg-IFN and RBV combination therapy. We also evaluated antiviral signaling induced by BCAA using an in vitro HCV replication system.

Materials and Methods

Patients

A total of 168 patients with CH-C at the Graduate School of Medicine at Kanazawa University Hospital (Kanazawa, Japan) and its related hospitals in Japan (Table 1, Supplementary Table 1) were evaluated in the present study. The clinical characteristics of these patients have been described previously.[4] All patients were administered Peg-IFN-alfa 2b (Schering-Plough K.K., Tokyo, Japan) and RBV combination therapy for 48 weeks. The definition of the treatment response was as follows: sustained viral response (SVR), clearance of HCV viremia 24 weeks after the cessation of therapy; transient response (TR), no detectable HCV viremia at the cessation of therapy but relapse during the follow-up period; and no response (NR). Genetic variation of the IL-28B polymorphism at rs8099917 was evaluated in all patients using TaqMan Pre-Designed SNP Genotyping Assays (Applied Biosystems, Carlsbad, CA) as described previously.[4] Gene expression profiling in the liver was performed in 91 patients using the Affymetrix Human 133 Plus 2.0 microarray chip (Affymetrix, Santa Clara, CA) as described previously (Supplementary Table 1).[4]

Plasma Amino Acid Analysis

Amino acid concentrations in plasma samples were measured by high-performance liquid chromatography–electrospray ionization–mass spectrometry, followed by derivatization.[11] Detailed experimental procedures are described in the Supplementary Materials and Methods section.

Culture Medium

Huh-7 and Huh-7.5 cells (kindly provided by Professor C. M. Rice, Rockefeller University, New York, NY) were maintained in Dulbecco's modified Eagle medium (DMEM; Gibco BRL, Gaithersburg, MD) containing 10%

fetal bovine serum and 1% penicillin/streptomycin (normal medium). Amino acid-free medium (ZERO medium) was prepared by mixing 5.81 g nutrition-free DMEM (Nacalai Tesque, Kyoto, Japan), 1.85 g NaHCO$_3$, 1 g glucose, and 0.5 mL 1M (mol/L) sodium pyruvate in 500 mL Milli-Q water, then sterilizing with a 0.22-μm filter (Millipore, Billerica, MA). Low amino acid media (×1/5, ×1/10, ×1/30, and ×1/100 DMEM) were prepared by diluting ×1 DMEM with ZERO medium. Powdered BCAA (leucine-isoleucine-valine, 2:1:1.2) (Ajinomoto Pharma, Tokyo, Japan) was freshly dissolved with distilled water at 100 mmol/L, then applied to cultured medium at 2 mmol/L, 4 mmol/L, or 8 mmol/L.

Western Blotting and Immunofluorescence Staining

A total of 1.5 × 10^5 Huh-7 cells were seeded in normal medium 24 hours before performing the experiments. The medium was changed to low-amino-acid medium and maintained for up to 24 hours. Western blotting was performed as previously described.[12] Cells were washed in phosphate-buffered saline (PBS) and lysed in RIPA buffer containing complete Protease Inhibitor Cocktail and PhosSTOP (Roche Applied Science, Indianapolis, IN). The membranes were blocked in Blocking One-P (Nacalai Tesque). The antibodies used for Western blotting are summarized in the Supplementary Materials and Methods section.

For immunofluorescence staining, cells were fixed with 4% paraformaldehyde in PBS, then permeabilized with 0.1% Triton-X 100 in PBS. The primary anti-forkhead box O (Foxo)3a antibody (Abcam, Cambridge, MA) was used at a final concentration of 2 μg/mL in PBS containing 2% fetal bovine serum at 4°C for 16 hours. Incubation with the Alexa Fluor 488–conjugated secondary antibody (Invitrogen, Carlsbad, CA) at a 500-fold dilution in PBS containing 3% fetal bovine serum antibody was performed for 4 hours, and cells were stained with Hoechst 33258 to visualize nuclear DNA (Vector Laboratories, Burlingame, CA).

Quantitative Real-Time Detection Polymerase Chain Reaction

A total of 1.5 × 10^5 Huh-7 cells were seeded in normal medium 24 hours before performing the experiments. The medium was changed to low-amino-acid medium, to which IFN-alfa and/or BCAA was added, and maintained for 24 hours. Rapamycin treatment (100 nmol/L) was performed for 30 minutes in normal medium before a medium change. RNA was isolated using TriPure isolation reagent (Roche Applied Science), and complementary DNA (cDNA) was synthesized using the High Capacity cDNA reverse transcription kit (Applied Biosystems, Carlsbad, CA). Real-time detection polymerase chain reaction (PCR) was performed using the 7500 Real-Time PCR System (Applied Biosystems) and Power SYBR Green PCR Master Mix (Applied Biosystems) containing specific primers according to the manufacturer's

Table 1. Comparison of Clinical Factors Between Patients With and Without NR

Clinical category	SVR+TR	NR	Univariate P value	Multivariate odds (95% CI)	Multivariate P value
Patients, n	125	43		—	
Age and sex					
Age, y	57 (30–72)	56 (30–73)	.927	—	
Sex, male vs female	68 vs 57	24 vs 19	.872	—	
Liver histology					
F stage (F1–2 vs F3–4)	95 vs 30	20 vs 23	.001	6.35 (2.02–23.7)	.001
A grade (A0–1 vs A2–3)	68 vs 57	19 vs 24	.248	—	
Host gene factors					
IL-28B (TT vs TG/GG)[a]	109 vs 12	12 vs 31	<.001	19.7 (5.74–82.7)	<.001
ISGs (Mx, IFI44, IFIT1), (<3.5 vs ≥3.5)	103 vs 22	12 vs 31	<.001	5.26 (1.65–17.6)	.005
Metabolic factors					
BMI, kg/m^2	23.2 (16.3–34.7)	23.4 (19.5–40.6)	.439	—	
TG, mg/dL	98 (30–323)	116 (45–276)	.058	—	
T-Chol, mg/dL	167 (90–237)	160 (81–214)	.680	—	
LDL-Chol, mg/dL	82 (36–134)	73 (29–123)	.019	—	
HDL-Chol, mg/dL	42 (20–71)	47 (18–82)	.098	—	
FBS, mg/dL	94 (60–291)	96 (67–196)	.139	—	
Insulin, μU/mL	6.6 (0.7–23.7)	6.8 (2–23.7)	.039	—	
HOMA-IR	1.2 (0.3–11.7)	1.2 (0.4–7.2)	.697	—	
Fischer ratio	2.3 (1.5–3.3)	2.1 (1.5–2.8)	.005	8.91 (1.62–55.6)	.011
Other laboratory parameters					
AST level, IU/L	46 (18–258)	64 (21–283)	.017	—	
ALT level, IU/L	60 (16–376)	82 (18–345)	.052	—	
γ-GTP level, IU/L	36 (4–367)	75 (26–392)	<.001	—	
WBC, /mm^3	4800 (2100–11100)	4800 (2500–8200)	.551	—	
Hb level, g/dL	14 (9.3–16.6)	14.4 (11.2–17.2)	.099	—	
PLT, ×104/mm^3	15.7 (7–39.4)	15.2 (7.6–27.8)	.378	—	
Viral factors					
ISDR mutations ≤1 vs ≥2	80 vs 44	34 vs 9	.070	4.12 (1.25–15.9)	.019
HCV-RNA, KIU/mL	2300 (126–5000)	1930 (140–5000)	.725	—	
Treatment factors					
Total dose administered					
Peg-IFN, μg	3840 (960–7200)	3840 (1920–2880)	.916	—	
RBV, g	202 (134–336)	202 (36–336)	.531	—	
Achieved administration rate					
Peg-IFN, %					
≥80%	84	28	.975	—	
<80%	42	14			
RBV (%)					
≥80%	76	24	.745	—	
<80%	50	18			
Achievement of EVR	101/125 (81%)	0/43 (0%)	<.001	—	

BMI, body mass index; CI, confidence interval; FBS, fasting blood sugar; γ-GTP, gamma-glutamyl transpeptidase; Hb, hemoglobin; HDL-chol, high density lipoprotein cholesterol; LDL-chol, low density lipoprotein cholesterol; PLT, platelets; T-chol, total cholesterol; TG, triglycerides; WBC, leukocytes.
[a]IL-28B SNP at rs8099917.

instructions. The primer sequence for real-time detection PCR is given in the Supplementary Materials and Methods section. HCV RNA was detected as described previously[12] and expression was standardized to that of glyceraldehyde-3-phosphate dehydrogenase.

Reporter Assay

Construction of the interferon stimulated response element (ISRE)-luc reporter plasmid and Socs3-luc or Socs3 (FoxO binding element mutant [FBEmut])-luc reporter plasmids is described in the Supplementary Materials and Methods section.

Huh-7 cells were transfected with the ISRE-luc reporter plasmid 24 hours before IFN-alfa treatment. Cells were treated with IFN-alfa (0 or 100 U/mL) and BCAA (2 mmol/L) in low-amino-acid media. After 24 hours, luciferase activities were measured using the Dual Luciferase assay system (Promega, Madison, WI). For Socs3 promoter activities, Huh-7 cells were transfected with Socs3-luc or Socs3 (FBEmut)-luc reporter plasmids together with the Foxo3a expression plasmid, and luciferase activities were measured after 24 hours. Values were normalized to the luciferase activity of the co-transfected pGL4.75 Renilla luciferase-expressing plasmid (Promega).

Knockdown Experiments

Huh-7 cells were transfected with Ctrl (Stealth RNAi Negative Control Low GC Duplex #2; Invitrogen) or

targets (regulatory associated protein of mTOR [Raptor] and Foxo3a) (Supplementary Materials and Methods) small interfering RNA (siRNA) using Lipofectamine RNAiMAX reagent (Invitrogen) according to the manufacturer's instructions. After 48 hours, cells were cultured in normal or low-amino-acid media for a further 24 hours. The knockdown effect was confirmed by Western blotting.

Chromatin Immunoprecipitation Assay

Detailed experimental procedures are described in the Supplementary Materials and Methods section.

HCV Replication Analysis

pH77S3 is an improved version of pH77S, a plasmid containing the full-length sequence of the genotype 1a H77 strain of HCV with 5 cell culture–adaptive mutations that promote its replication in Huh-7 hepatoma cells.[13] pH77S.3/Gaussia luciferase (GLuc)2A is a related construct in which the GLuc sequence, fused to the 2A autocatalytic protease of foot-and-mouth virus RNA, was inserted in-frame between p7 and NS2[14] (Supplementary Materials and Methods). A signal sequence in GLuc directs its secretion into cell culture media, allowing real-time, dynamic measurements of GLuc expression to be performed without the need for cell lysis.

A 10-μg aliquot of synthetic RNA transcribed from pH77S.3/GLuc2A was used for electroporation. Cells were pulsed at 260 V and 950 μF using the Gene Pulser II apparatus (Bio-Rad Laboratories, Hercules, CA) and plated in fresh normal medium for 12 hours to recover. Cell medium was changed to ×1 DMEM without serum for 8 hours, then changed to low-amino-acid medium containing 0–8 mmol/L BCAA for a further 24 hours. Cells and culture medium were collected and used for GLuc assays, real-time detection PCR, and Western blotting. The number of viable cells was determined by a (3-[4,5-dimethylthiazol-2-yl]-5-[3-carboxymethoxyphenyl]-2-[4-sulfophenyl] -2H-tetrazolium, inner salt) assay (Promega).

Continuously JFH-1–infecting Huh-7 cells were obtained by the infection of Huh-7 cells with JFH-1 cell culture-derived HCV at a multiplicity of infection of 0.01. Cells were maintained in normal medium by passaging every 3–4 days for approximately 6 months. About 20%–30% of the cells consistently were positive for HCV core protein (Supplementary Figure 4). Culture medium of JFH-1–infecting Huh-7 cells was changed to the low-amino-acid medium containing 0–8 mmol/L BCAA for 24 hours. Cells then were collected and used for assays.

Statistical Analysis

Results are expressed as mean ± standard deviation. Significance was tested by 1-way analysis of variance with the Bonferroni method, and differences were considered statistically significant at a P value of less than .05.

Results

Fischer's Ratio as a Predictive Factor for Treatment Response

The clinical characteristics of patients who received Peg-IFN and RBV combination therapy are shown in Table 1 and Supplementary Table 1, and explanations of these characteristics have been described previously.[4] All patients were infected with HCV genotype 1b and had a high viral load (>100 IU/mL). We compared patients with SVR + TR against those with NR, as assessed by the overall plausibility of treatment response groups using Fisher's C statistic as previously described.[4] We included data on the IL-28B polymorphism and plasma amino acid composition (aminogram).

Univariate regression analysis showed that no single amino acid was associated significantly with treatment response; however, using Fischer's ratio, the BCAA (Ile+Leu+Val)/aromatic amino acids (Phe+Tyr) ratio was associated significantly with treatment response (P = .005) (Table 1). Of the 121 patients with IL-28B major type, SVR, TR, and NR were observed in 53%, 37%, and 10%, respectively, and among 33 patients with IL-28B minor type, SVR, TR, and NR were observed in 15%, 17%, and 68%, respectively (P < .001) (data not shown). Fischer's ratio of SVR, TR, and NR was 2.35 ± 0.38, 2.30 ± 0.29, and 2.10 ± 0.31, respectively (P < .015) (data not shown).

We selected IL-28B polymorphism, hepatic ISG expression, fibrosis stage, HCV RNA, interferon sensitivity determining region mutation, and Fischer's ratio as factors for multivariate analysis. Multivariate analysis revealed that the minor type of IL-28B polymorphism (TG or GG at rs8099917) (odds ratio, 19.7; P < .001), advanced fibrosis stage of the liver (F3–4) (odds ratio, 6.35; P = .001), high hepatic ISGs (≧3.5) (odds ratio, 5.26; P = .005), low Fischer's ratio (continuous range, 1.5–3.3) (unit odds, 8.91; P = .011), and presence of ISDR mutation (≦1) (odds ratio, 4.12; P = .019) independently contributed to NR (Table 1).

The distribution of the Fischer's ratio according to fibrosis stage is shown in Supplementary Figure 1. The ratio decreased significantly in advanced fibrosis stage (F3–4) compared with early fibrosis stage (F1). No significant association between major or minor type of IL-28B polymorphism and different fibrosis stages of the liver was observed (Supplementary Figure 1A). In early fibrosis (F1–2) (Supplementary Figure 1B), 90% (80 of 89) of SVR+TR cases had the major type of IL-28B polymorphism, and 94% (16 of 17) of NR cases had the minor type. However, in the advanced fibrosis stage of the liver (F3–4) (Supplementary Figure 1C), 85% (23 of 27) of SVR+TR cases had the major type of IL-28B polymorphism and 50% (10 of 20) of NR cases had the minor type. Thus, in advanced fibrosis stages, factors other than the IL-28B polymorphism appear to contribute to NR. Interestingly, the Fischer's ratio was significantly lower in NR patients than SVR+TR pa-

tients in the advanced fibrosis stage of the liver. There-fore, Fischer's ratio could be an important predictor for NR that is independent of IL-28B polymorphism and histologic stage of the liver.

Fischer's Ratio and mTORC1 Signaling in CH-C Livers

Hepatic gene expression in 91 of 168 patients (Supplementary Table 1) was obtained using Affymetrix genechip analysis as described previously.[4] To examine the relationship between the plasma Fischer's ratio and mTORC1 signaling in the liver we evaluated the expression of key regulatory genes related to mTORC1 signaling. We found that expression of branched chain amino-acid transaminase 1 (BCAT1), an important catalytic enzyme of BCAA, was significantly negatively correlated with Fischer's ratio (Figure 1A). This indicates that the plasma Fischer's ratio is regulated in the liver as well as in peripheral muscle. Interestingly, the expression of c-myc, a positive regulator of BCAT1 (Figure 1C),[15] was correlated negatively with the Fischer's ratio (Figure 1B). The expres-sion of PDCD4, a negative transcriptional target of ribo-somal p70 S6 protein kinase (S6K), downstream of mTORC1, was correlated significantly with BCAT1 (Fig-ure 1D and E). Thus, in CH-C livers, BCAT1 is induced with progressive liver disease and mTORC1 signaling is repressed, a process that might involve c-myc. Fischer's ratio of the plasma therefore can be seen to reflect mTORC1 signaling in the liver.

Impaired IFN Signaling in Huh-7 Cells Grown in Low-Amino-Acid Medium

Recent reports have shown the functional rele-vance of mTOR on IFN signaling and antiviral re-sponses.[9,10] To evaluate IFN-alfa signaling and the mTOR pathway, we used Huh-7 cells grown in different amino acid conditions ($\times 1$ DMEM, $\times 1/5$ DMEM, $\times 1/30$ DMEM, and $\times 1/100$ DMEM). The phosphorylated forms of mTOR (p-mTOR) and S6K (pS6K), an important downstream regulator of mTORC1 signaling, were de-creased substantially in $\times 1/30$ DMEM and $\times 1/100$ DMEM (Figure 2A). Interestingly, the expression of the phosphorylated form of signal transducer and activator of transcription 1 (pSTAT1), an essential transducer of type 1 IFN signaling, also was decreased in these conditions (Figure 2A). Similarly, the expression of p-mTOR and pSTAT1 was repressed significantly in CH-C livers with a low Fischer's ratio compared with those with a high Fischer's ratio (Sup-plementary Figure 2, Supplementary Table 2).

To examine whether decreased pSTAT1 expression might be owing to repressed mTORC1 signaling, we knocked down the expression of Raptor, a specific subunit of mTORC1. We achieved more than 50% knockdown of Raptor by specific siRNA (Figure 2B). Under these condi-tions, the expression of p-mTOR and pSK6 were re-pressed, which is consistent with previous reports.[16] The expression of pSTAT1 also was repressed after Raptor knockdown (Figure 2B).
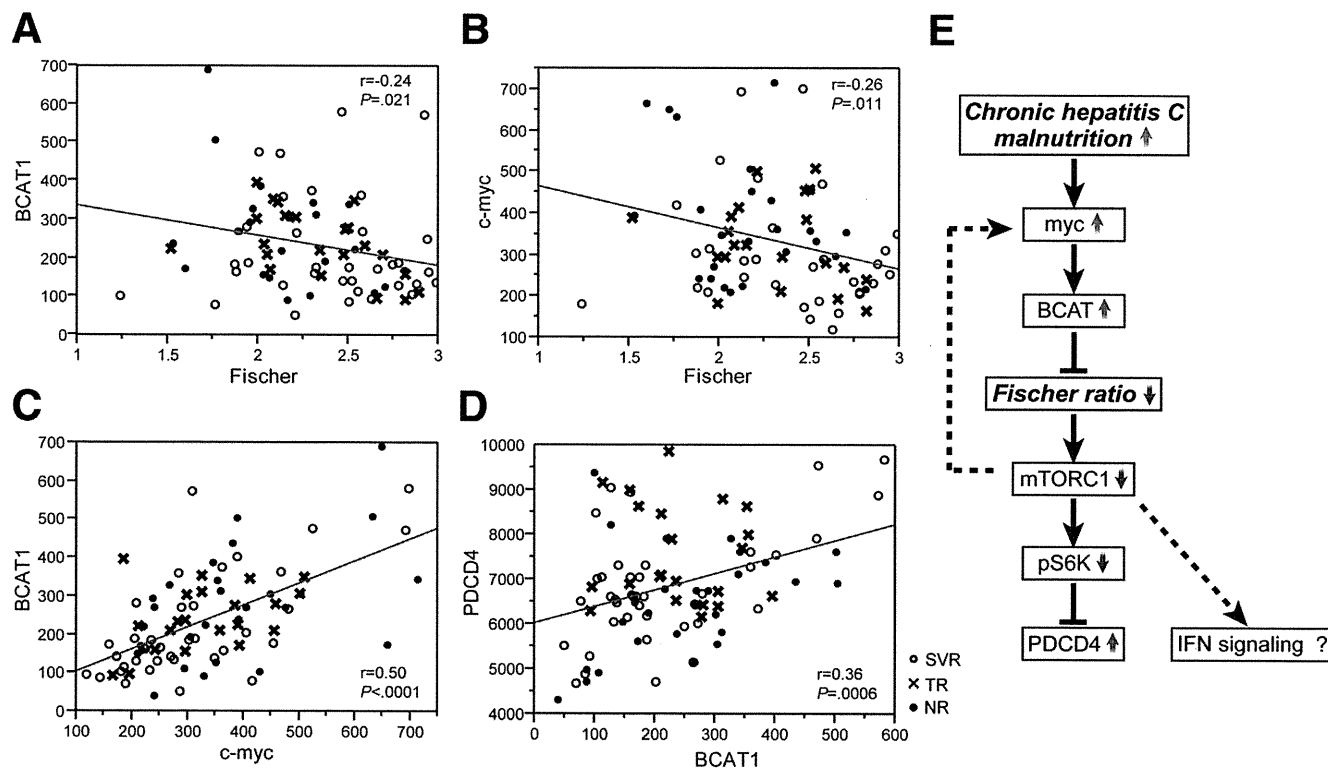
Figure 1. Regression analysis of mTORC1-related gene expression in liver. Gene expression values were determined by probe intensities. (A) BCAT1 and Fischer's ratio. (B) c-myc and Fischer's ratio. (C) BCAT1 and c-myc. (D) PDCD4 and BCAT1. (E) Putative signaling of mTORC1-related genes in CH-C.
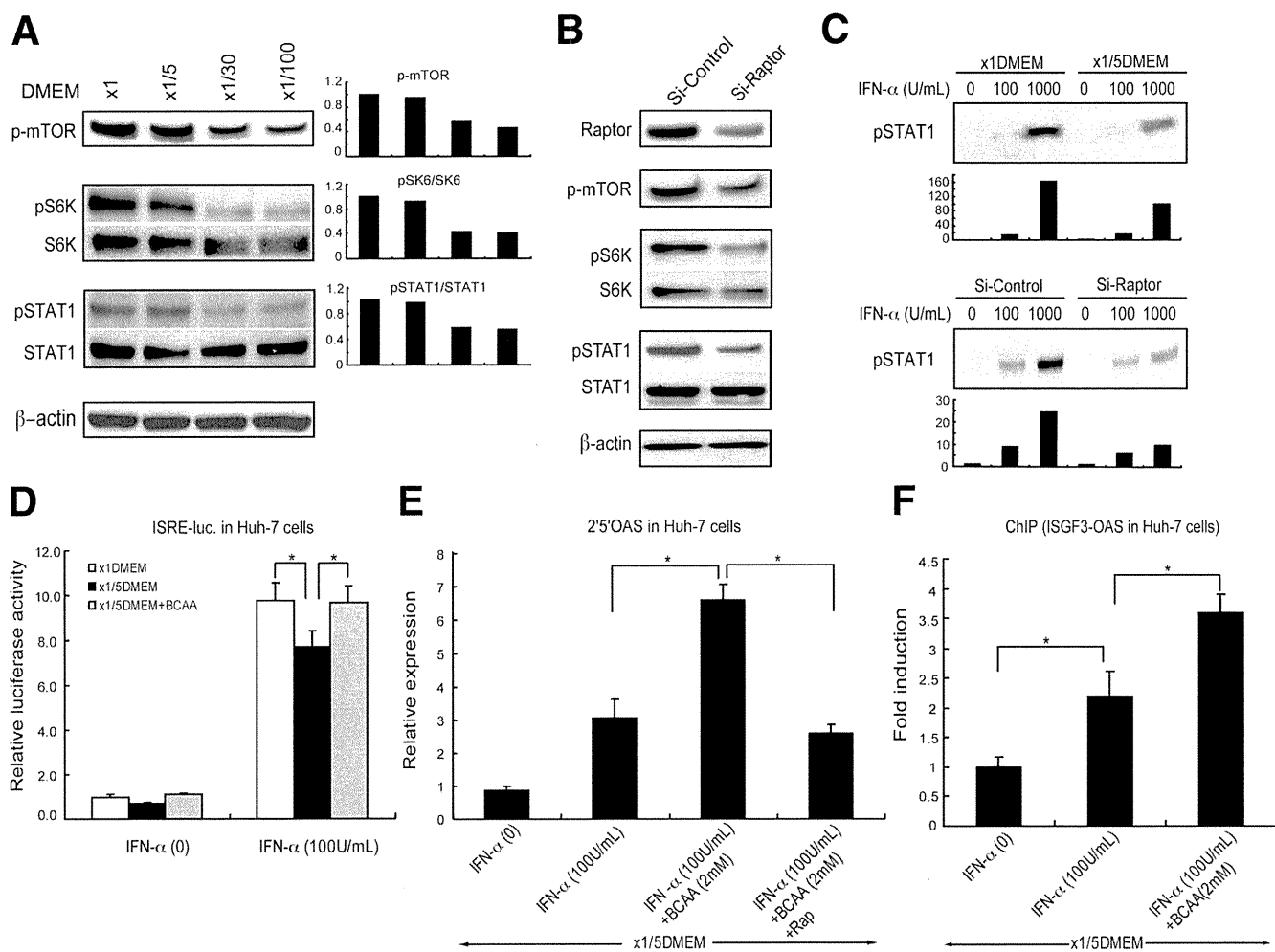
Figure 2. mTORC1 and IFN signaling in Huh-7 cells in low-amino-acid medium. (*A*) p-mTOR, pS6K, and pSTAT1 expression in different amino acid media. (*B*) p-mTOR, pS6K, and pSTAT1 expression under Raptor knock-down conditions. (*C*) IFN-alfa stimulation and pSTAT1 expression in low-amino-acid media or under Raptor knock-down conditions. (*D*) IFN-alfa stimulation and ISRE reporter activities in normal and low-amino-acid media. (*E*) IFN-alfa stimulation and 2'5'OAS expression supplemented with BCAA or rapamycin in low-amino-acid medium. (*F*) Chromatin immunoprecipitation of 2'5'OAS promoter region by ISGF3γ.

The induction of pSTAT1 by IFN-alfa (1000 U/mL) stimulation was impaired in ×1/5 DMEM or in Raptor knocked-down condition, compared with the control (Figure 2*C*). Consistent with these results, IFN-alfa–induced ISRE-dependent transcriptional activity, as measured using an ISRE-luciferase reporter assay, was impaired significantly in ×1/5 DMEM compared with ×1 DMEM (Figure 2*D*). However, this activity could be rescued by the addition of 2 mmol/L BCAA (Figure 2*D*). These results were confirmed by determining the expression of the endogenous IFN-alfa responsive gene, 2'5'OAS, using quantitative reverse-transcription PCR. Figure 2*E* shows that BCAA treatment augmented 2'5'OAS expression in low levels of amino acids, and that this could be reversed by the addition of rapamycin, an inhibitor of mTORC1 (Figure 2*E*). Furthermore, chromatin immunoprecipitation (ChIP) experiments revealed that transcriptional augmentation by BCAA was mediated by the binding of the IFN-alfa–inducible transcription factor, ISGF3γ, to the promoter region of 2'5'OAS (Figure 2*F*). These results indicate that

amino acids in culture media play an essential role in IFN-alfa signaling through mTORC1 signaling, and that the addition of BCAA can overcome impaired IFN-alfa signaling in Huh-7 cells.

Induction of Socs3 in Low-Amino-Acid Medium in Huh-7 Cells

Besides being involved in mTOR signaling, Foxo transcriptional factors mediate another important branch of nutrition-sensing signaling pathway.[17] Therefore, we evaluated forkhead box O3A (Foxo3a) expression in low-amino-acid conditions in Huh-7 cells. After 6 hours culture in ×1/5, ×1/30, and ×1/100 DMEM, expression of the phosphorylated form of Foxo3a (pFoxo3a) decreased, whereas that of total Foxo3a increased in ×1/5 and ×1/30 DMEM, and the ratio of pFoxo3a to Foxo3a (pFoxo3a/Foxo3a) substantially decreased (Figure 3*A* and *B*). It has been reported that dephosphorylated Foxo3a is translocated to the nucleus before activation of its target genes.[18] In the present study, immunofluorescent staining
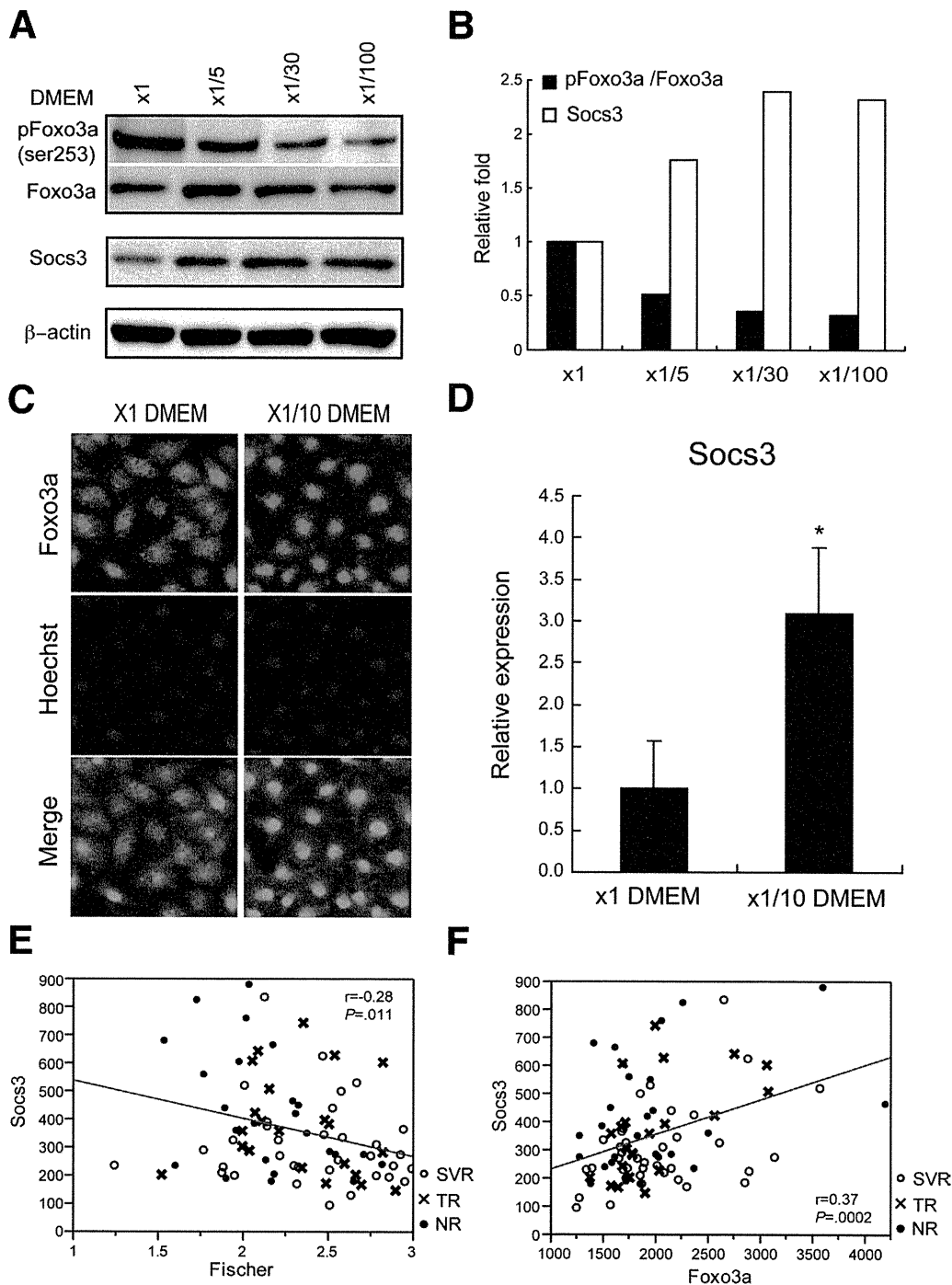
Figure 3. Foxo3a and Socs3 signaling in Huh-7 cells in low-amino-acid medium. (A) Foxo3a and Socs3 expression in different amino acid media. (B) Relative change of pFoxo3a/Foxo3a and Socs3 expression in different amino acid media. (C) Immunofluorescence staining of Foxo3a in Huh-7 cells in normal and low-amino-acid media. (D) Relative change of Socs3 messenger RNA in Huh-7 cells in normal and low-amino-acid media. (E) Regression analysis of Socs3 in liver and Fischer's ratio. (F) Regression analysis of Socs3 and Foxo3a in liver.

with an anti-Foxo3a antibody showed that Foxo3a diffused in both the cytoplasm and nucleus in normal amino acid medium, but localized in the nucleus in low-amino-acid medium (×1/10 DMEM) (Figure 3C).

Interestingly, in low-amino-acid medium, transcription and protein expression of Socs3 increased significantly (Figure 3A, B, and D). The induction of Socs3 in a state of malnutrition also was confirmed in clinical samples. In CH-C livers there was a significant negative correlation between the plasma Fischer's ratio and Socs3 expression, implying that Socs3 expression increases during the malnutrition state induced by CH-C. There was also a significant correlation between Foxo3a and the transcriptional level of Socs3 in CH-C livers (Figure 3E and F), suggesting an in vitro and in vivo biological role for Foxo3a in the activation of Socs3 expression. These findings also were confirmed by Western blotting of CH-C livers (Supplementary Figure 2, Supplementary Table 2).

Socs3 Is a Transcriptional Target of Foxo3a

The significant correlation between Socs3 and Foxo3a in CH-C livers prompted us to analyze the Socs3 promoter sequence and, in doing so, we identified a putative Foxo binding element (FBE) (Figure 4A). To investigate the functional relevance of Foxo3a in the transcriptional regulation of Socs3, we constructed reporter plasmids containing a luciferase coding region fused to the Socs3 promoter region (Socs3-luc). Socs3-luc promoter activity was increased substantially by the overexpression of Foxo3a (Figure 4B). The mutations introduced in the putative FBE (FBEmut) in the Socs3 promoter significantly reduced Foxo3a-induced Socs3 promoter activation (Figure 4B).

Foxo3a then was knocked down by siRNA and Socs3 induction was evaluated. After suppression of Foxo3a (Supplementary Figure 3), Socs3 promoter activity was repressed significantly in low-amino-acid medium ($\times 1/10$ DMEM) (Figure 4C). Thus, Foxo3a appears to be indispensable for activating the Socs3 promoter under low-amino-acid conditions. Correlating with these results, ChIP assays using an anti-Foxo3a antibody showed a significant increase in the association between Foxo3a and the FBE of the Socs3 promoter in low-amino-acid conditions ($\times 1/10$ DMEM) (Figure 4D). Taken together, these results suggest that, besides mTORC1 signaling, the Foxo3a-mediated Socs3 signaling pathway might contribute to impaired IFN signaling in a state of malnutrition in CH-C. BCAA potentially restores this signaling (Figure 4E).

Effect of BCAA on HCV Replication in Huh-7 or Huh-7.5 Cells

Based on the earlier-described results, we used 2 HCV in vitro replication systems to examine whether BCAA affects HCV replication in Huh-7 or Huh-7.5 cells. The first system used a recombinant infectious genotype 1a clone, H77S.3/GLuc2A (Supplementary Materials and Methods, Supplementary Figure 4), including reporter genes, whereas the second used continuously JFH-1–infecting Huh-7 cells (Supplementary Materials and Methods).

The synthetic RNA transcribed from pH77S.3/GLuc2A was introduced into Huh-7.5 cells and replication of H77S.3/GLuc2A was evaluated in normal or low-amino-acid medium supplemented with BCAA. H77S.3/GLuc2A increased significantly by 2.6-fold in Huh-7.5 cells grown in low-amino-acid medium ($\times 1/5$ DMEM) compared with normal amino acid medium ($\times 1$ DMEM). Interestingly, BCAA repressed H77S.3/GLuc2A replication in a dose-dependent manner (Figure 5A). In agreement with these results, the expression of Mx-1 was increased significantly by the addition of BCAA (Figure 5B). Similar findings were observed in JFH-1–infecting Huh-7 cells (Materials and Methods, Supplementary Figure 4). Although no obvious increase in HCV replication was observed in low-amino-acid medium ($\times 1/5$ DMEM) compared with normal amino acid medium ($\times 1$ DMEM), JFH-1 replication was repressed significantly by the addition of BCAA in a dose-dependent manner (Figure 5D). The expression of Mx-1 was increased substantially by the addition of BCAA (Figure 5E), suggesting that BCAA significantly repressed HCV replication in cells with either naive or persistent HCV infection. Importantly, there were no significant differences in cell viability between the conditions (Figure 5C and F).

To validate these findings, signaling pathways in HCV replicating cells were examined (Figure 6A and B). BCAA increased pS6K in a dose-dependent manner, implying its involvement in the activation of mTORC1 signaling. Related to this, expression of pSTAT1 was shown to be increased and the ratio of pSTAT1 to total STAT1 (pSTAT1/STAT1) increased 2.5- to 3-fold after the addition of BCAA. Thus, BCAA activated mTORC1 and the JAK-STAT signaling pathway in HCV-infected cells. In addition, the expression ratio of pFoxo3a to total Foxo3a (pFoxo3a/Foxo3a) increased 3- to 4-fold, indicating an increase in the cytoplasmic form of Foxo3a that is exposed to proteasome degradation. Concordant with these findings, we observed a decrease in the expression of Socs3. In addition, expression of the HCV core protein decreased as shown in Figure 6A and B. Thus, these results clearly show that BCAA repressed HCV replication through activation of IFN signaling and repression of Socs3-mediated IFN inhibitory signaling, as proposed in Figure 4E.

Discussion

Thompson et al[5] showed that the IL-28B polymorphism, HCV RNA, nationality (Caucasian/Hispanic vs African American), hepatic fibrosis stage, and fasting blood sugar level are all significant variables for achieving SVR in patients infected with genotype 1 HCV. However, the significance of variable factors for treatment response in conjunction with the IL-28B polymorphism has not been evaluated fully. In the present study, in addition to previously examined variables,[4] we included the plasma Fischer's ratio as a nutritional parameter. Multivariate analysis showed that the minor type of IL-28B polymorphism, advanced fibrosis stage, high hepatic ISGs, low Fischer's ratio, and ISDR mutation (≤ 1) independently contributed to NR (Table 1). Interestingly, among patients of similar fibrosis stage (F3–4), the Fischer's ratio was significantly lower in NR than SVR+TR cases. Therefore, the plasma value of Fischer's ratio was associated with the treatment response that was independent of the IL-28B polymorphism and histologic stage of the liver, although patients with advanced hepatic fibrosis are likely to be nutritionally affected.

As a nutrient sensor signaling pathway, the protein kinase mTOR plays an essential role in maintaining homeostasis and regulates protein synthesis in response to nutrient conditions. mTOR is the catalytic subunit of 2 distinct complexes, mTORC1 and mTORC2. In addition

A

Socs3 promoter

```
Human  --CGCCCTCG GCGCCCGCGG CCCCTCCCTC ACCCTCCGCG CTCAGCCTTT CTCTGCTGCG
          |  | || |  |||||||| |||||||||| |||||||||| | |||||||||| |  |||    |
Mouse  TCCAAGCCCG CCCTCCGCGG CCCCTCCCTC GCCCTCCGCG CACAGCCTTT CAGTGC--AG
```

```
                  FBE                                GAS
       AGTAGTGACT AAACATTACA AGAAGGCCGG CCGCGCAGTT CCAGGAATCG GGGGGCGGGG
       ||||||||||  | |||||||||| ||||| |||| ||| ||| || |||||||| ||| ||||||||||
       AGTAGTGACT AAACATTACA AGAAGACCGG CCGGGCAGTT CCAGGAATCG GGGGGCGGGG
                                               Transcription start site
```

```
                TATA
       CGCGGCGGCC GCCTATATAC CCGCGAGCGC GGCCTCCGCG GCGGCTC
       ||    |||| |  |  || ||| ||||| |||| |||||||| | |||||||
       CGTACTGGCC GGGTAAATAC CCGCGCGCGC GGCCTCCGAG GCGGCTC
```
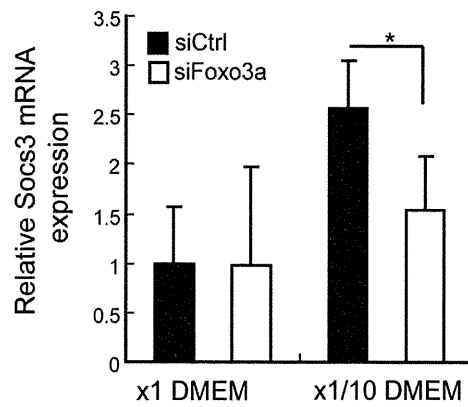
FBE of Socs3 promoter
  Wild seq.   **TGACTAAACATTACA**
  Mutated seq.   **TGACTCACCATTACA**
  Consensus seq. **(G/A)TAAA(T/C)A**

B
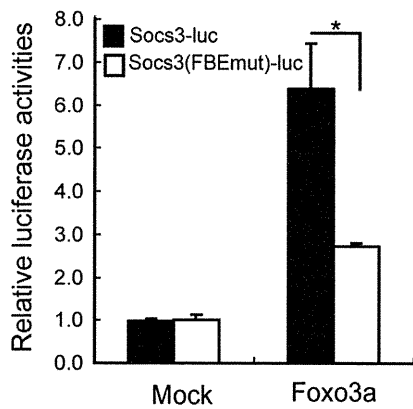
C

D

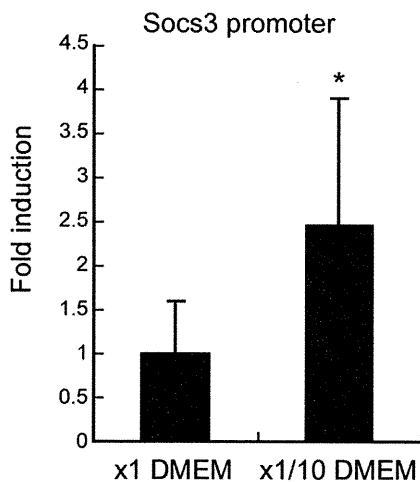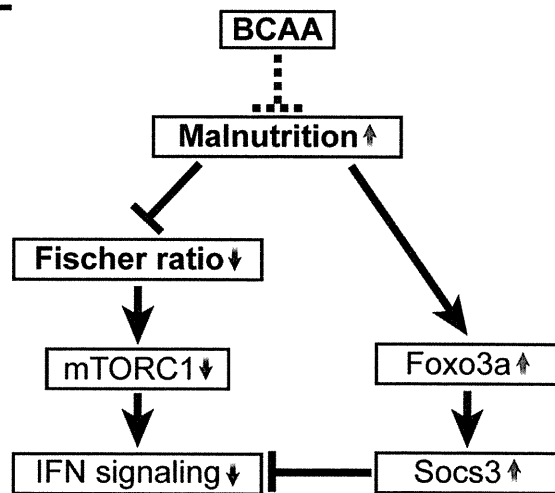## E

Figure 4. Socs3 promoter assay. (*A*) Primary structure of putative Foxo binding element in Socs3 promoter region. (*B*) Socs3-luc and Socs3 (FBEmut)-luc activities after overexpression of Foxo3a in Huh-7 cells. (*C*) Relative Socs3 messenger RNA (mRNA) expression after knockdown of Foxo3a in normal and low-amino-acid media. (*D*) Chromatin immunoprecipitation of Socs3 promoter region by Foxo3a in normal and low-amino-acid media. (*E*) Model of impaired IFN signaling by repressed mTORC1 signaling and increased Socs3 signaling under CH-C state of malnutrition.
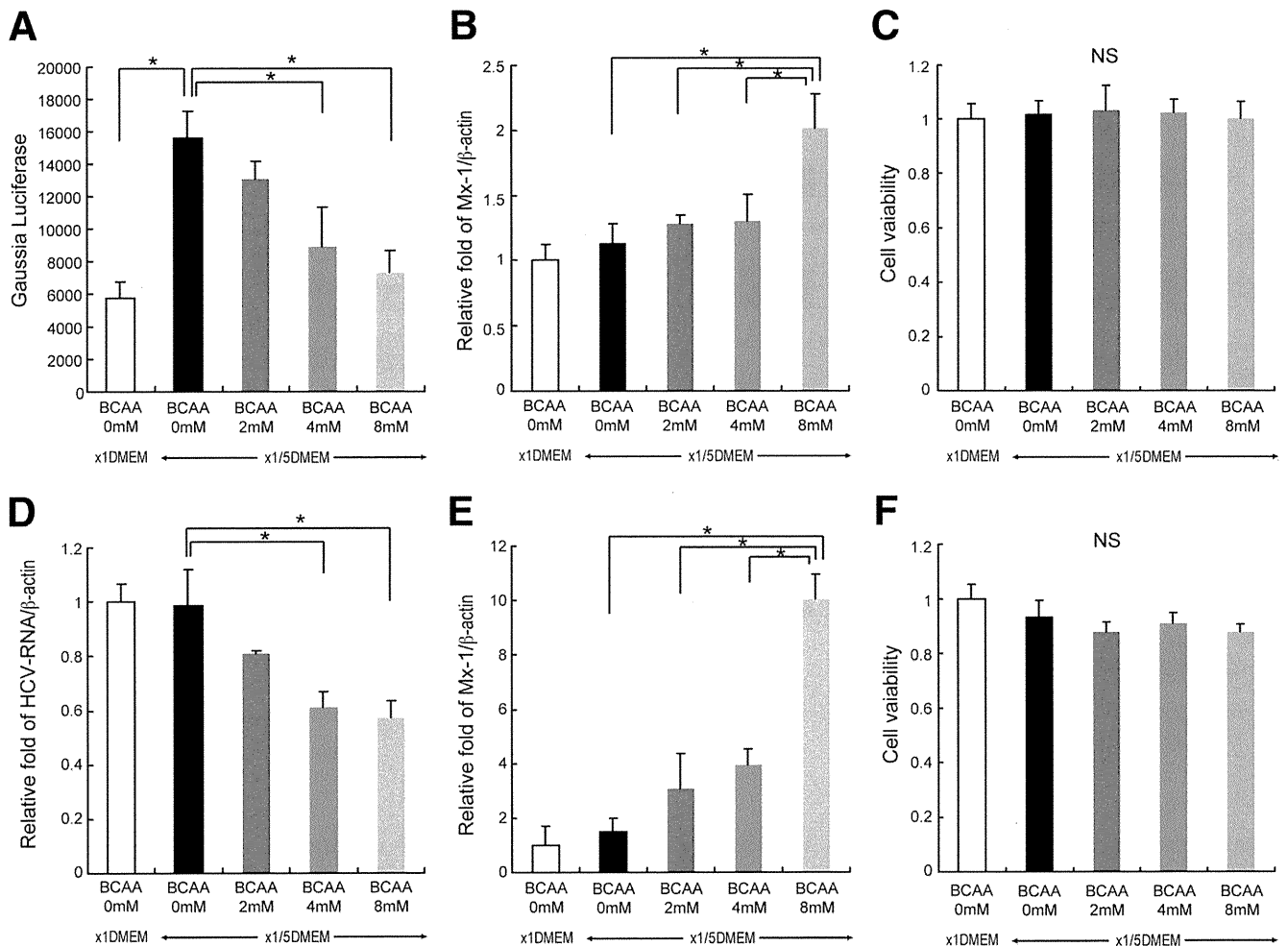
Figure 5. Effect of BCAA on HCV replication in cells in low-amino-acid medium. (*A*) Effect of BCAA on H77S.3/GLuc2A replication in Huh-7.5 cells. (*B*) Mx-1 expression in H77S.3/GLuc2A-transfected Huh-7.5 cells supplemented with BCAA. (*C*) Viability of Huh-7.5 cells. (*D*) Effect of BCAA on JFH-1 replication continuously infecting Huh-7 cells. (*E*) Mx-1 expression in continuously JFH-1–infecting Huh-7 cells supplemented with BCAA. (*F*) Viability of Huh-7 cells.

to these metabolic aspects, recent reports have shown that mTORC1 participates in IFN signaling and antiviral defense responses,[9,10] although the precise signaling pathway has not yet been clarified. In the present study, we evaluated mTORC1 signaling in CH-C livers using gene expression profiling of 91 patients (Figure 1, Supplementary Table 1). We observed a significant negative correlation between plasma Fischer's ratio and hepatic expression of BCAT1, an important catalytic enzyme of BCAA (Figure 1*A*). Moreover, BCAT1 expression was correlated positively with PDCD4 expression, which in turn is regulated negatively by pS6K at the transcriptional level (Figure 1*D*).[16] Thus, the expression of BCAT1 appears to be a negative indicator of mTORC1 signaling in the liver, and the plasma Fischer's ratio is partially reflected by mTORC1 signaling in the liver and muscle.

Interestingly, the expression of c-myc was correlated significantly with BCAT1 (Figure 1*C*) as reported previously.[15] Several studies observed up-regulated c-myc expression in advanced stages of CH-C[19] but, on the other hand, c-myc recently was shown to be a target of

mTORC1 in hepatic cells.[17] The existence of a feedback mechanism between c-myc and mTORC1 signaling to maintain liver homeostasis (Figure 1*E*) is plausible, although the precise mechanisms need to be confirmed.

Impaired mTORC1 signaling is suggested to affect the IFN-alfa–induced signaling pathway. To address this, the relationship between mTORC1 and IFN signaling was assessed using a cell culture system. In low-amino-acid medium ($\times 1/5$, $\times 1/30$, and $\times 1/100$ DMEM), expression of pSTAT1 was decreased substantially, correlating with the impaired mTORC1 signaling represented by decreased p-mTOR and pS6K expression in Huh-7 cells (Figure 2*A*).

The relationship between mTORC1 and IFN signaling was confirmed further by the knock-down experiment of Raptor, a specific subunit of mTORC1 (Figure 2*B*), although a more precise analysis should be performed to confirm this relationship. Importantly, when Huh-7 cells were stimulated by IFN-alfa, pSTAT1 induction was repressed significantly in low-amino-acid medium ($\times 1/5$ DMEM) or in Raptor knocked-down conditions (Figure 2*C*). It therefore could be speculated that IFN treat-
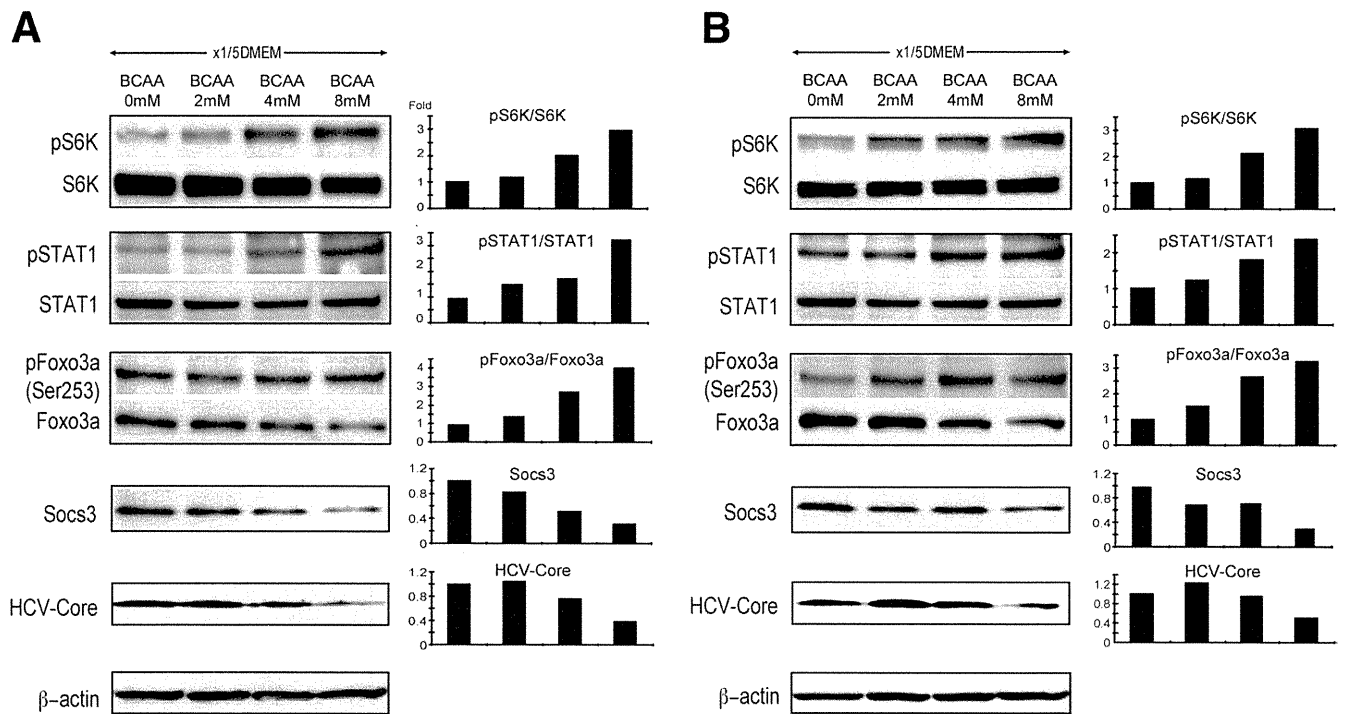
Figure 6. Expression of S6K, STAT1, Foxo3a, Socs3, and HCV core in H77S.3/GLuc2A-transfected Huh-7.5 cells or continuously JFH-1–infecting Huh-7 cells supplemented with BCAA.

ment of patients with liver malnutrition and impaired mTORC1 signaling would lead to reduced induction of ISGs. Importantly, BCAA was able to restore impaired IFN signaling through increased binding of ISGF3γ to its targets (Figure 2D–F).

Besides cross-talk of mTORC1 and IFN signaling, we revealed that Foxo3a also is involved in the IFN inhibitory pathway. In low-amino-acid medium, expression of pFoxo3a (ser253) was decreased substantially whereas that of Socs3 was increased. A decreased pFoxo3a/Foxo3a ratio indicates nuclear accumulation of Foxo3a before activation of its target genes, and this was confirmed by immunofluorescent staining (Figure 3C). The expression of Foxo3a was significantly positively correlated with that of Socs3 in CH-C liver (Figure 3F). These findings prompted us to identify a putative FBE in the Socs3 promoter region (Figure 4A). In fact, Socs3 promoter reporter activity was activated by overexpression of Foxo3a, and mutation of FBE impaired Foxo3a-dependent Socs3 promoter activation. Conversely, induction of Socs3 was not observed when expression of Foxo3a was knocked down by siRNA in low-amino-acid medium. Socs3 induction in low-amino-acid medium was owing to increased binding of Foxo3a to the FBE, which was confirmed by ChIP (Figure 4D). Therefore, in addition to impaired mTORC1 signaling, the Foxo3a-mediated Socs3 IFN inhibitory pathway might be involved in impaired IFN signaling in patients with liver malnutrition (Figure 4E).

Finally, we examined whether BCAA could restore impaired IFN signaling and inhibit HCV replication in cells

under conditions of malnutrition. Importantly, BCAA could repress replication of the recombinant genotype 1a-derived HCV, H77S.3/GLuc2A, in a dose-dependent manner (Figure 5A). H77S.3/GLuc2A RNA produces infectious virus[14] and, therefore, the results indicate that BCAA might act on a naive HCV infection. Moreover, BCAA inhibited JFH-1–infected Huh-7 cells in which JFH-1 continuously was infecting in a dose-dependent manner. These results indicate that BCAA had an inhibitory effect on either naive or persistent HCV infection irrespective of genotypes (1a and 2a). Consistent with these results, BCAA induced the expression of pSTAT1 and Mx protein in a dose-dependent manner, and repressed Socs3 expression through increasing the ratio of pFoxo3a (ser243) to Foxo3a in a dose-dependent manner (Figures 5 and 6). Therefore, BCAA potentially could restore impaired IFN signaling and inhibit HCV replication in a CH-C state of malnutrition.

In conclusion, we addressed the clinical significance of the nutritional state of the liver on the treatment response of Peg-IFN and RBV combination therapy for CH-C. Although further studies are required to fully define the precise mechanisms underlying mTOR and IFN signaling, we showed that plasma values of Fischer's ratio are a useful nutritional parameter associated with treatment response. Fischer's ratio reflects mTORC1 signaling in the liver, which is correlated with IFN signaling and related to Socs3 IFN inhibitory signaling through Foxo3a. The potential usefulness of BCAA for the augmentation of IFN signaling could suggest a new therapeutic application for advanced-stage CH-C.

Supplementary Material

Note: To access the supplementary material accompanying this article, visit the online version of *Gastroenterology* at www.gastrojournal.org, and at doi: 10.1053/j.gastro.2011.03.051.

Appendix A

The Hokuriku Liver Study Group is composed of the following members: Drs Takashi Kagaya, Kuniaki Arai, Kaheita Kakinoki, Kazunori Kawaguchi, Hajime Takatori, and Hajime Sunakosaka (Department of Gastroenterology, Kanazawa University Graduate School of Medicine, Kanazawa, Japan); Drs Touru Nakahama and Shinji Kamiyamamoto (Kurobe City Hospital, Kurobe, Toyama, Japan); Dr Yasuhiro Takemori (Toyama Rosai Hospital, Uozu, Toyama, Japan); Dr Hikaru Oguri (Koseiren Namerikawa Hospital, Namerikawa, Toyama, Japan); Drs Yatsugi Noda and Hidero Ogino (Toyama Prefectural Central Hospital, Toyama, Japan); Drs Yoshinobu Hinoue and Keiji Minouchi (Toyama City Hospital, Toyama, Japan); Dr Nobuyuki Hirai (Koseiren Takaoka Hospital, Takaoka, Toyama, Japan); Drs Tatsuho Sugimoto and Koji Adachi (Tonami General Hospital, Tonam, Toyama, Japan); Dr Yuichi Nakamura (Noto General Hospital, Nanao, Ishikawa, Japan); Drs Masashi Unoura and Ryuhei Nishino (Public Hakui Hospital, Hakui, Ishikawa, Japan); Drs Hideo Morimoto and Hajime Ohta (National Hospital Organization Kanazawa Medical Center, Kanazawa, Ishikawa, Japan); Dr Hirokazu Tsuji (Kanazawa Municipal Hospital, Kanazawa, Ishikawa, Japan); Drs Akira Iwata and Shuichi Terasaki (Kanazawa Red Cross Hospital, Kanazawa, Ishikawa, Japan); Drs Tokio Wakabayashi and Yukihiro Shirota (Saiseikai Kanazawa Hospital, Kanazawa, Ishikawa, Japan); Drs Takeshi Urabe and Hiroshi Kawai (Public Central Hospital of Matto Ishikawa, Hakusan, Ishikawa, Japan); Dr Yasutsugu Mizuno (Nomi Municipal Hospital, Nomi, Ishikawa, Japan); Dr Shoni Kameda (Komatsu Municipal Hospital, Komatsu Ishikawa, Japan); Drs Hirotoshi Miyamori and Uichiro Fuchizaki (Keiju Medical Center, Nanao, Ishikawa, Japan); Dr Haruhiko Shyugo (Kanazawa Arimatsu Hospital, Kanazawa, Ishikawa, Japan); Dr Hideki Osaka (Yawata Medical Center, Komatsu, Ishikawa, Japan); Dr Eiki Matsushita (Kahoku Central Hospital, Tsubata, Ishikawa, Japan); Dr Yasuhiro Katou (Katou Hospital, Komatsu, Ishikawa, Japan); Drs Nobuyoshi Tanaka and Kazuo Notsumata (Fukuiken Saiseikai Hospital, Fukui, Japan); Dr Mikio Kumagai (Kumagai Clinic, Tsuruga, Fukui, Japan); and Dr Manabu Yoneshima (Municipal Tsuruga Hospital, Tsuruga, Fukui, Japan).

References

1. Fried MW, Shiffman ML, Reddy KR, et al. Peginterferon alfa-2a plus ribavirin for chronic hepatitis C virus infection. N Engl J Med 2002;347:975–982.

2. Tanaka Y, Nishida N, Sugiyama M, et al. Genome-wide association of IL28B with response to pegylated interferon-alpha and ribavirin therapy for chronic hepatitis C. Nat Genet 2009;41: 1105–1109.

3. Ge D, Fellay J, Thompson AJ, et al. Genetic variation in IL28B predicts hepatitis C treatment-induced viral clearance. Nature 2009;461:399–401.

4. Honda M, Sakai A, Yamashita T, et al. Hepatic ISG expression is associated with genetic variation in interleukin 28B and the outcome of IFN therapy for chronic hepatitis C. Gastroenterology 2010;139:499–509.

5. Thompson AJ, Muir AJ, Sulkowski MS, et al. Interleukin-28B polymorphism improves viral kinetics and is the strongest pretreatment predictor of sustained virologic response in genotype 1 hepatitis C virus. Gastroenterology 2010;139:120–129 e18.

6. Nishitani S, Ijichi C, Takehana K, et al. Pharmacological activities of branched-chain amino acids: specificity of tissue and signal transduction. Biochem Biophys Res Commun 2004;313:387–389.

7. Matsumura T, Morinaga Y, Fujitani S, et al. Oral administration of branched-chain amino acids activates the mTOR signal in cirrhotic rat liver. Hepatol Res 2005;33:27–32.

8. Kim DH, Sarbassov DD, Ali SM, et al. mTOR interacts with raptor to form a nutrient-sensitive complex that signals to the cell growth machinery. Cell 2002;110:163–175.

9. Colina R, Costa-Mattioli M, Dowling RJ, et al. Translational control of the innate immune response through IRF-7. Nature 2008;452: 323–328.

10. Kaur S, Lal L, Sassano A, et al. Regulatory effects of mammalian target of rapamycin-activated pathways in type I and II interferon signaling. J Biol Chem 2007;282:1757–1768.

11. Shimbo K, Kubo S, Harada Y, et al. Automated precolumn derivatization system for analyzing physiological amino acids by liquid chromatography/mass spectrometry. Biomed Chromatogr 2009; 24:683–691.

12. Shirasaki T, Honda M, Mizuno H, et al. La protein required for internal ribosome entry site-directed translation is a potential therapeutic target for hepatitis C virus replication. J Infect Dis 2010;202:75–85.

13. Yi M, Villanueva RA, Thomas DL, et al. Production of infectious genotype 1a hepatitis C virus (Hutchinson strain) in cultured human hepatoma cells. Proc Natl Acad Sci U S A 2006;103:2310–2315.

14. Shimakami T, Welsch C, Yamane D, et al. Protease inhibitor-resistant hepatitis C virus mutants with reduced fitness from impaired production of infectious virus. Gastroenterology 2011; 140:667–675.

15. Eden A, Simchen G, Benvenisty N. Two yeast homologs of ECA39, a target for c-Myc regulation, code for cytosolic and mitochondrial branched-chain amino acid aminotransferases. J Biol Chem 1996; 271:20242–2045.

16. Dowling RJ, Topisirovic I, Alain T, et al. mTORC1-mediated cell proliferation, but not cell growth, controlled by the 4E-BPs. Science 2010;328:1172–1176.

17. Teleman AA, Hietakangas V, Sayadian AC, et al. Nutritional control of protein biosynthetic capacity by insulin via Myc in Drosophila. Cell Metab 2008;7:21–32.

18. Zhang X, Gan L, Pan H, et al. Phosphorylation of serine 256 suppresses transactivation by FKHR (FOXO1) by multiple mechanisms. Direct and indirect effects on nuclear/cytoplasmic shuttling and DNA binding. J Biol Chem 2002;277: 45276–45284.

19. Farinati F, Cardin R, Bortolami M, et al. Oxidative damage, proinflammatory cytokines, TGF-alpha and c-myc in chronic HCV-related hepatitis and cirrhosis. World J Gastroenterol 2006;12: 2065–2069.

CLINICAL LIVER

CLINICAL LIVER

Reprint requests
Address requests for reprints to: Shuchi Kaneko, MD, PhD, Department of Gastroenterology, Graduate School of Medicine, Kanazawa University, Takara-Machi 13-1, Kanazawa 920-8641, Japan. e-mail: skaneko@m-kanazawa.jp; e-mail: fax: (81) 76-234-4250.